

INFORMATION TO USERS

THIS DISSERTATION HAS BEEN
MICROFILMED EXACTLY AS RECEIVED

This copy was produced from a microfiche copy of the original document. The quality of the copy is heavily dependent upon the quality of the original thesis submitted for microfilming. Every effort has been made to ensure the highest quality of reproduction possible.

PLEASE NOTE: Some pages may have indistinct print. Filmed as received.

Canadian Theses Division
Cataloguing Branch
National Library of Canada
Ottawa, Canada K1A 0N4

AVIS AUX USAGERS

LA THESE A ETE MICROFILMEE
TELLE QUE NOUS L'AVONS RECUE

Cette copie a été faite à partir d'une microfiche du document original. La qualité de la copie dépend grandement de la qualité de la thèse soumise pour le microfilmage. Nous avons tout fait pour assurer une qualité supérieure de reproduction.

NOTA BENE: La qualité d'impression de certaines pages peut laisser à désirer. Microfilmée telle que nous l'avons reçue.

Division des thèses canadiennes
Direction du catalogage
Bibliothèque nationale du Canada
Ottawa, Canada K1A 0N4

ULTIMATE STRENGTH OF ORTHOGONAL GRID SPACE TRUSSES

Nicholas Iliadis

A THESIS
in
The Faculty
of
Engineering

Presented in Partial Fulfillment of the Requirements for
the Degree of Master of Engineering at
Concordia University
Montréal, Québec, Canada

November 1975

ABSTRACT

ABSTRACT

Nicholas Liadis

ULTIMATE STRENGTH OF ORTHOGONAL GRID SPACE TRUSSES

This thesis reports a comparison between theoretical predictions and experimental results for the ultimate strength and behaviour of orthogonal grid space trusses loaded to collapse.

The theoretical analysis used two approaches, a simplified method treating the truss as a continuum, and a computer solution, using an elastic stiffness method.

The basic assumption on the load/shortening relationship of struts is examined.

A number of trusses have been tested monotonically to failure with different point supports and spans.

The experimental results showed that the ultimate load approached the predicted load for collapse. However, the failure of the test trusses occurred without buckling of the chord members, which suggests that the distribution of loads in the chords moves towards that predicted for the collapse state, as a result of both slippage and other sources of non-linearity.

ACKNOWLEDGEMENTS

ACKNOWLEDGEMENTS

I wish to place on record my sincere thanks and gratitude to Professor C. Marsh for his suggestions and guidance throughout this project.

I would also like to take this opportunity of expressing my thanks to Professor Z.A. Zielinski for his encouragement during my studies.

Thanks also are due to the members of the Structures Laboratory of Concordia University under the direction of Mr. L. Stankevicius.

TABLE OF CONTENTS

TABLE OF CONTENTS

	<u>PAGE</u>
ABSTRACT	i
ACKNOWLEDGEMENTS	ii
LIST OF TABLES	v
LIST OF FIGURES	vi
NOTATIONS	ix
I INTRODUCTION	1
II A REVIEW OF THE LITERATURE	6
III THEORETICAL ANALYSIS FOR THE ULTIMATE LOAD FOR ORTHOGONAL GRID SPACE TRUSSES	9
3.1 Introduction	9
3.2 Analysis Treating the Truss as a Continuum Using an Energy Method	9
3.2.1 Case 1. Boundaries Supported	9
3.2.2 Case 2. Corners Supported (Test Case)	15
3.2.2.1 Analysis of a first model	18
3.2.2.2 Analysis of a second model	20
3.2.3 Conflicts in the Method Treating the Truss as a Continuum	22
3.3 Computer Analysis	27
IV CHORD BEHAVIOUR	31
V TEST MODELS OF ORTHOGONAL SPACE TRUSSES	39
5.1 Introduction	39
5.1.1 Description of the Test models	41
5.2 Theoretical Analysis of the Test Models	46
5.2.1 Analysis According to Simple Energy Method	46
5.2.2 Analysis of Test Model According to the Computer Method vs. the Energy Method	49

	<u>PAGE</u>
VI CONDUCT OF TEST - TEST RESULTS	54
6.1 Test Set-Up	54
6.2 Instrumentation	54
6.2.1 Load Measurements	54
6.2.2 Deformation Measurements	55
6.3 Testing Procedure	55
6.4 Test Results	56
6.4.1 Model 1	56
6.4.2 Model 2	58
6.4.3 Model 3	59
VII DISCUSSION OF TEST RESULTS	60
7.1 Test 1	61
7.2 Test 2	62
7.3 Test 3	63
VIII CONCLUSIONS	65
REFERENCES	67
APPENDIX A - Diagrams, Tables and Figures Illustrating the Behaviour of the Test Models. . .	68

LIST OF TABLES

LIST OF TABLES

<u>NUMBER</u>	<u>DESCRIPTION</u>	<u>PAGE</u>
3.1	Comparison of continuum analysis and computer solution for orthogonal grid space trusses supported at four points and uniformly loaded	30
5.1	Tension and compression capacities of the members used in the test models	47
<u>Appendix A</u>		
A.1	Measured vertical deflections of joints 45,71,76,48 of first test model	74
A.2	Strain-gage readings for members along the assumed yield lines of first test	75
A.3	Vertical deflections of joints 45,71,76,48 of first test model according to computer analysis	81
A.4	Measured vertical deflections of joints 45,71,76,55 of second test model	88
A.5	Vertical deflections of joints 45,71,76,48 of second test model according to computer analysis	89
A.6	Vertical deflections of joints 27,49,35,53 of third test model according to computer analysis	95
A.7	Measured vertical deflections of joints 27,49,35,53 of third test model	96


LIST OF FIGURES

LIST OF FIGURES

<u>FIGURE</u>	<u>DESCRIPTION</u>	<u>PAGE</u>
1.1	Orthogonal grid space truss	2
1.2	Yield lines for orthogonal grid truss edges supported and uniformly loaded	4
1.3	Yield lines for plates, edges supported and uniformly loaded	4
3.1	Load-shortening relationship assumed for struts	10
3.2	Collapse mechanism for orthogonal grid truss, supported along the edges, and loaded uniformly	11
3.3	Cross-section of an orthogonal grid space truss	13
3.4	Collapse mode assumed for test truss type one. (Model 1)	16
3.5	Collapse mode assumed for test truss type two. (Model 2)	17
3.6	Rotation angle along the yield lines of type one model	19
3.7	Rotation angle along the yield lines of type two model	21
3.8	Collapse mechanism for orthogonal grid truss, supported at the corners and uniformly loaded	23
3.9	Forces and moments acting in a quarter of the truss in Fig. 3.8 in collapse state	24
3.10	Assumed yield zones for collapse state to satisfy static equilibrium	26
4.1	Typical load-shortening relationships for struts	32
4.2	Ideal load-shortening relationships for struts	35

<u>FIGURE</u>	<u>DESCRIPTION</u>	<u>PAGE</u>
4.3	Comparing between ideal load-shortening relationships for struts and experimental results	37
4.4	Ideal load-axial deformation curve for tension members	38
5.1	Details of M-dec system	40
5.2	Details of chords and diagonals used for the test trusses	42
5.3	First test model, supported at A and loaded at B. (Quarter of the surface). Depth of the grid 9.5"	43
5.4	Second test model, (quarter of the surface). Depth of the grid 9.5"	44
5.5	Third test model (quarter of the surface). Depth of the grid 9.5"	45
5.6	Comparison between ideal load-shortening relationships for struts and experimental results for a chord	51
<u>Appendix</u>		
A.1	Illustration of the reinforced diagonals in first test model	68
A.2	Sequence of member failure for first test model according to ultimate computer analysis	69
A.3	Sequence of member failure for second test model according to ultimate computer analysis	70
A.4	Sequence of member failure for third test model according to ultimate computer analysis	71
A.5	Method of load application to test models	72
A.6	Location of strain-gages at first test model	73
A.7	Failure of first test model	82

<u>FIGURE</u>	<u>DESCRIPTION</u>	<u>PAGE</u>
A.8	Forces in the members along the assumed yield lines of the first test model	83
A.9	Load vertical deflection curves for joints 45,48,71,76 of first test model, according to computer analysis and experimental results	84
A.10	Load-vertical deflection curves for joints 45,71,76,55 of second test model according to computer analysis and experimental results	90
A.11	Failure of second test model	94
A.12	Load-vertical deflection curves for joints 27,49,35,53 of third test model according to computer analysis and experimental results	97



NOTATIONS

NOTATIONS

x, y, z	Cartesian coordinates, z-axis normal to plane of plate
a, b, l	dimensions of space truss or elements
c	distance to extreme fiber
d	truss depth
q	load/unit area
r	radius of gyration
s	spacing of chords
A	cross-section area of a strut
E	energy dissipated in yield lines, elastic modulus
I	moment of inertia
K	numerical factor
L	length
M_o	"plastic" moment per unit length
P	axial load in struts, concentrated load applied at the joints of the truss
P_t, P_c	capacities in tension and compression, respectively
P_e	Euler load
Q	Total applied load on the truss
U	loss of potential energy
δ	vertical deflections of joints of space truss, shortening of a strut
Δ	central bow in a strut
ϵ	axial strain
σ	mean axial stress

σ_e

Euler stress

σ_y

yield stress

CHAPTER I
INTRODUCTION

CHAPTER I

INTRODUCTION

The Department of Civil Engineering at Concordia University, is currently engaged in a research programme to determine the ultimate capacity of orthogonal grid space trusses. Space trusses are a popular way of spanning large areas with few intermediate supports. This is understandable because these structures provide a form of roof construction combining low cost with an esthetically pleasing appearance. A feature of such trusses is that the basic pattern is repeated a large number of times.

In Figure 1.1 an orthogonal grid truss is illustrated. The sets of upper and lower chords form square grids, while the diagonals form pyramids.

The growing popularity of double-layer grids is due to a number of distinct advantages of this form of construction. They can be listed as follows:

- (1) The structures are statically indeterminate and buckling of a compression member does not necessarily lead to the collapse of the whole framework.
- (2) The great rigidity of double-layer structures leads to relatively small deflections.

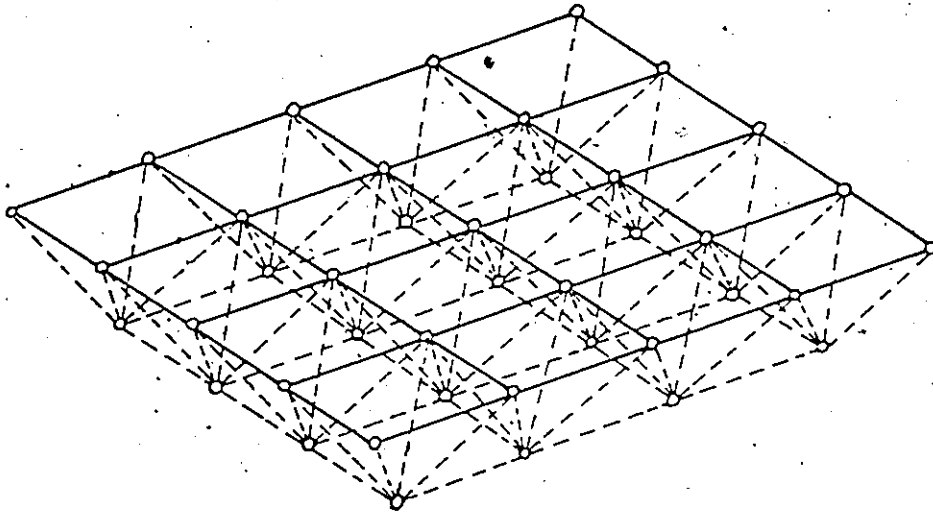


FIG. 1.1 ORTHOGONAL GRID SPACE TRUSS

- (3) Double-layered grids are characterized by an almost random location of loading and supports.
- (4) The space between the top and bottom layers of the grid can be used for location of the mechanical and electrical services.
- (5) The usual uniformity without the main and secondary beams is esthetically pleasing.

Linear elastic analysis of large space truss structures has become relatively routine and inexpensive, due to modern computational techniques, however, collapse load considerations are not as straightforward.

Since many space truss systems have been developed as standard products utilizing the maximum number of identical parts in order to minimize the cost, this study considers trusses with uniform chords and diagonals, respectively. Under these conditions, the collapse load consideration is more meaningful.

Orthogonal grid space trusses behave as two-way trusses, not as plates, since the upper and lower surfaces in the square grids possess no shear rigidity. The difference in the behaviour between a square truss and a plate when uniformly loaded to collapse and supported along the edges, is that the square truss fails along the lines

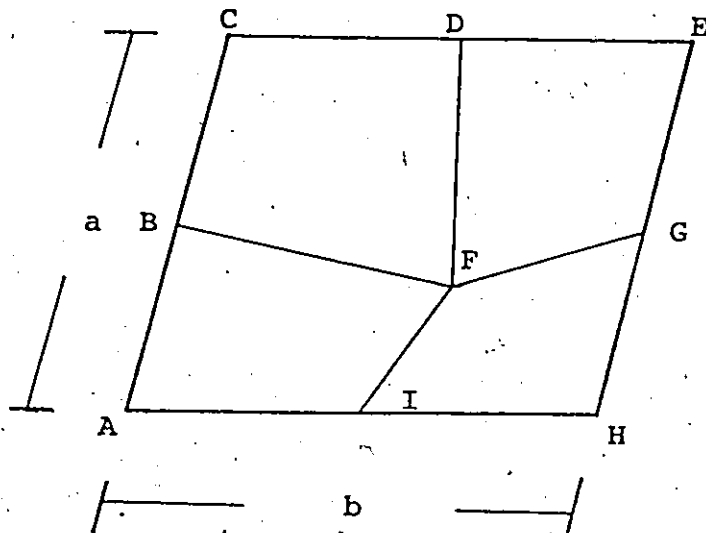


FIG. 1.2 YIELD LINES FOR ORTHOGONAL GRID TRUSS, EDGES SUPPORTED, AND UNIFORMLY LOADED

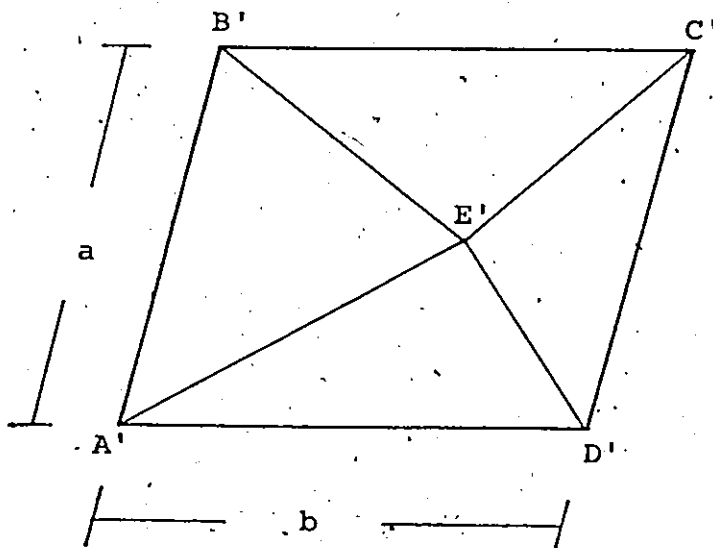


FIG. 1.3 YIELD LINES FOR PLATES, EDGES SUPPORTED, AND UNIFORMLY LOADED

shown in Fig. 1.2, and not along the diagonal lines (Fig. 1.3) as in the cases of steel plates and concrete slabs. This is because the surfaces (ABFI), (BFDC), (DEGF), (FGHI) of the truss can twist, while the surfaces (E'C'B'), (C'E'D'), (A'E'D'), (A'E'B') of the plate remain flat, thus, from geometrical considerations, we obtain the yielding lines which are illustrated in Fig. 1.3.

A simple analysis, using the energy method based on kinematically admissible collapse modes, gives design expression for the ultimate load. This expression is compared with the computer solutions and experimental results. The procedure in the computer programme is similar to that used by Wang [1] for rigid frames and Shin [2] for space trusses.

CHAPTER II
A REVIEW OF THE LITERATURE

CHAPTER II

A REVIEW OF THE LITERATURE

In this Chapter, the previous work on orthogonal grid space trusses is reviewed.

The literature recording the various aspects of grid space frame systems, is quite extensive. For instance, reference [3] contains most of the available information dealing with the elastic behaviour of such space frames. However, in spite of the well-recognized merits of limit state designs, relatively little effort has been made to extend the applications of the plastic methods of analysis to the ultimate-load design.

Some works on orthogonal grid space trusses have eliminated the large amount of computer time required for the analysis, which is especially true when truss is composed of a large number of members, by replacing the truss with an equivalent plate.

Timoshenko [4], made the statement that the differential equations of a plate and grillage are identical if the spacing between the beams is small, compared with the overall dimensions.

Flower and Schmidt [5] considered this aspect, and it has been shown that in the interior of the truss the differential equations of a plate with zero torsional

rigidity are the limiting form of the truss equation as the mesh size goes to zero, but has not estimated the error due to a finite grid size, nor a useful theoretical treatment of the influence of the boundary conditions. In the same study, it was shown that the truss forces (at the chords), are relatively independent of the web rigidity, whereas the deflections are more sensitive to this.

Suzuki et al [6] made an analysis of orthogonal grid space trusses based on differential equations.

Flower and Schmidt [7] again, in order to reduce the dimensionality (degrees of freedom) of the truss, investigated a method which converted a truss into an equivalent one with reduced dimensionality and which roughly corresponds to the behaviour of the initial truss.

Schmidt [8] tried to investigate an analysis of an orthogonal space truss, based on the "strip-method". However, for the truss considered by Schmidt, the development of compressive membrane action is significant and the application of the method is invalid. Schmidt then proposes a two-stage plastic design, based on the strip method that overcomes the effect of membrane forces.

For the ultimate capacity of an orthogonal space truss examined by Dickie and Dunn [9], the assumption was that the members which buckle can carry, after buckling, 10% of their maximum capacity, while the tension members can

carry, after yielding, the maximum force, so that a redistribution of forces will occur in the unyielding members. A number of trusses were analyzed on this basis, and also with the yield line approach. The results from the analysis are questionable, since for a truss with uniform members, the initial yield occurred at a load factor of 1, while the collapse did not occur until the load factor reached 3.38. This is known to be excessive. On the other hand, some trusses with varying member sizes yielded along the diagonal lines. This is of questionable economical value.

Mezzina et al [10] also reported the elastoplastic behaviour of a steel double layer space grid model, supported at its four corners.

The experimental results do not predict the behaviour of the truss when it is loaded more than the elastic limit, nor is it explained how the theoretical analysis gave an ultimate capacity for the structure 50% more than the elastic capacity, with the assumption that the members which buckle are not able to carry any load after this point.

Marsh [11] investigated a simple theoretical method for an ultimate analysis of orthogonal grid space trusses.

The present work is based on these investigations of Professor Marsh and also the compared experimental and theoretical results.

CHAPTER III

THEORETICAL ANALYSIS FOR THE ULTIMATE
LOAD FOR ORTHOGONAL GRID SPACE-TRUSSES

CHAPTER III

THEORETICAL ANALYSIS FOR THE ULTIMATE
LOAD FOR ORTHOGONAL GRID SPACE-TRUSSES3.1 INTRODUCTION

The most common cases of orthogonal space trusses, in practice, are those which have point supports or boundary supports parallel to the chord lines. In the analysis, it is assumed that the upper and lower chords have uniform cross-section and, further, that:

- (1) Any "flat" portion of the space truss can twist.
- (2) The chords in "unyielded" zones remain straight.
- (3) The tension members yielding and struts buckling have a "plateau" in the load/change of length relationship of sufficient extent to permit full redistribution of moments. (Fig. 3.1).

3.2 ANALYSIS TREATING THE TRUSS AS A
CONTINUUM USING AN ENERGY METHOD3.2.1 Case 1. Boundaries Supported

Consider the truss in Fig. 3.2, which is supported along the boundaries (AB), (BC), (CD), (DA).

Assume that a uniform load q per unit area is applied on the truss, and that it is the ultimate load. The

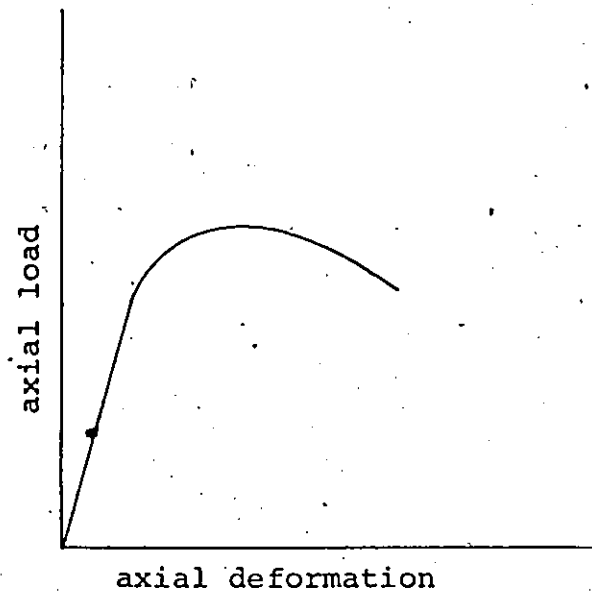


FIG. 3.1 LOAD-SHORTENING RELATIONSHIP ASSUMED FOR STRUTS

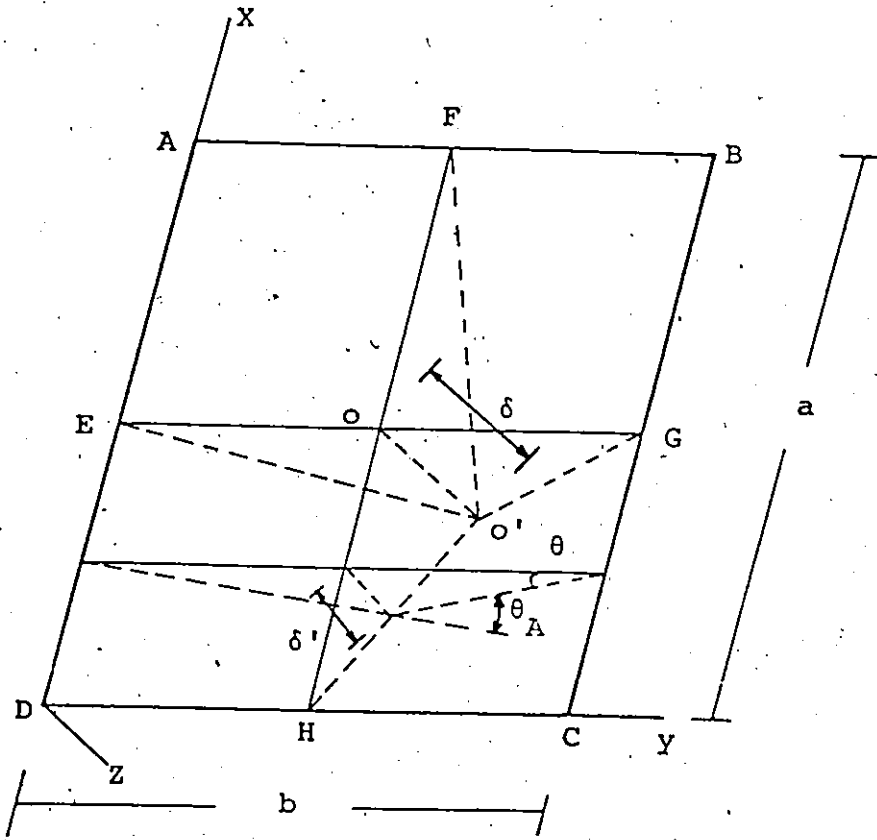


FIG. 3.2 COLLAPSE MECHANISM FOR ORTHOGONAL GRID TRUSS SUPPORTED ALONG THE EDGES AND LOADED UNIFORMLY

truss will yield along the lines (EO), (GO), (FO), (HO), because the truss has no torsional rigidity, while the boundaries (AB), (BC), (DC), (DA), will remain undeflected. The central point of the truss will drop down a distance δ . There will be a plastic moment (M_o) per unit length along the yielding lines (EO), (FO), (GO), (HO). This plastic moment (Fig. 3.3) is given by:

$$M_o = \frac{pd}{s} \quad (3.1)$$

where d = depth of the grid
 s = the space between the chords
 p = the ultimate capacity of the chords in tension or in compression

The mathematical expression for the surfaces (i.e., FBGO) after the deformation is:

$$z = \frac{4xy\delta}{ab} \quad (3.2)$$

Hence, the work done by the external apply load q per unit area is:

$$U = 4 \int_0^{a/2} \int_0^{b/2} qz \, dx dy = 4 \int_0^{a/2} \int_0^{b/2} \delta q \frac{4xy}{ab} \, dx dy = q\delta ab/4 \quad (3.3)$$

The total applied load Q is:

$$Q = q \, ab \quad (3.4)$$

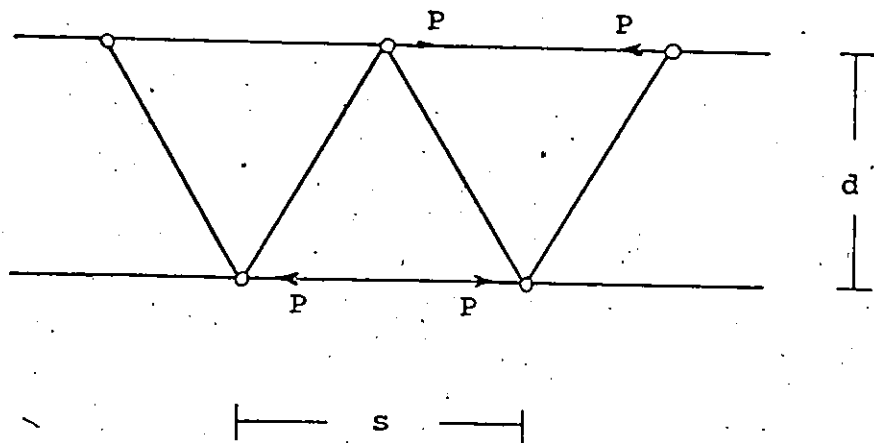


FIG. 3.3 . CROSS-SECTION OF AN ORTHOGONAL GRID SPACE TRUSS

Hence,

$$U = Q\delta/4 \quad (3.5)$$

The energy dissipated in yielding lines is a function of the plastic moment M_0 per unit length and of the rotation along the yielding lines (EO), (OG), (FO), (OH).

By referring to Fig. (3.2), the change in angle θ_A between the surfaces (OHCG) and (EOHD) along the yield line OH is:

$$\theta_A = 2\theta = 2(\delta'/\frac{b}{2}) = \frac{4\delta'}{b} \quad (3.6)$$

but

$$\delta' = \frac{x\delta}{\frac{a}{2}} = \frac{2\delta x}{a} \quad (3.7)$$

Hence

$$\theta_A = \frac{8\delta x}{ab} \quad (3.8)$$

and, the energy dissipated along the yield lines (HO) and (OF) is:

$$E_1 = 2M_0 \int_0^{a/2} \theta_A dx = 2M_0 \int_0^{a/2} \frac{8\delta x}{ab} dx = \frac{2M_0 \delta a}{b} \quad (3.9)$$

Similarly, the change in angle θ_B between the surfaces, along the yield lines (EO) and (OG) is given by:

$$\theta_B = \frac{8\delta y}{ab} \quad (3.10)$$

and the energy dissipated is:

$$E_2 = 2M_0 \int_0^{b/2} \theta_B dy = 2M_0 \int_0^{b/2} \frac{8\delta y}{ab} dy = \frac{2M_0 \delta b}{a} \quad (3.11)$$

The total dissipated energy is:

$$E = E_1 + E_2 = 2M_0 \delta \left(\frac{a}{b} + \frac{b}{a} \right) \quad (3.12)$$

Equating the work done from the applied load q and the energy dissipated in the yield lines, Eq.(3.5) and (3.12), gives:

$$V = E$$

$$\therefore \frac{Q\delta}{4} = 2M_0 \delta \left(\frac{a}{b} + \frac{b}{a} \right)$$

$$\therefore Q = 8M_0 \left(\frac{a}{b} + \frac{b}{a} \right)$$

For $a = b$

$$Q = 16M_0 \quad (3.13)$$

From Eq.(3.13) the ratio of the total applied ultimate load over the plastic moment per unit length for a space truss with supports on all sides, is 16.

3.2.2 Case 2. Corners supported (Test Case)

The space truss models which have been tested, in order to compare theoretical and experimental results, were supported at the four corners (or at four symmetrical joints close to the corners) and were loaded at four symm-

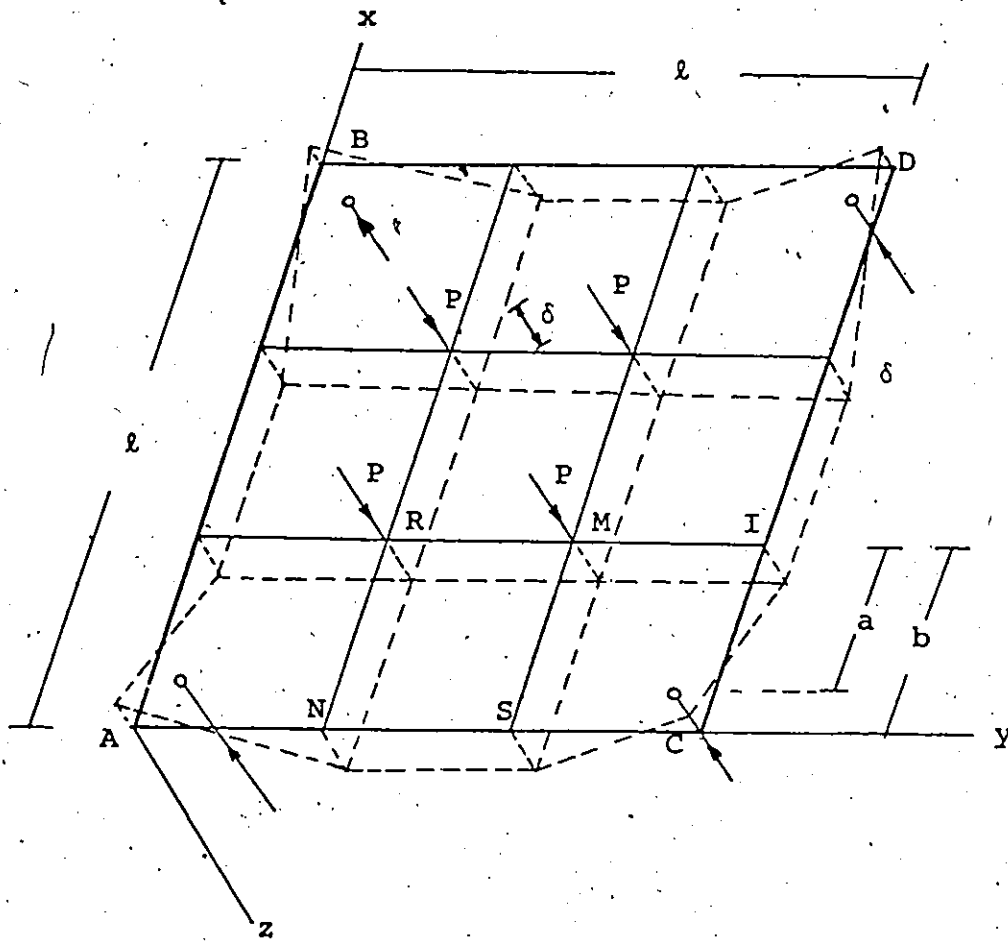


FIG. 3.4 COLLAPSE MODE ASSUMED FOR TEST TRUSS TYPE ONE (MODEL 1)

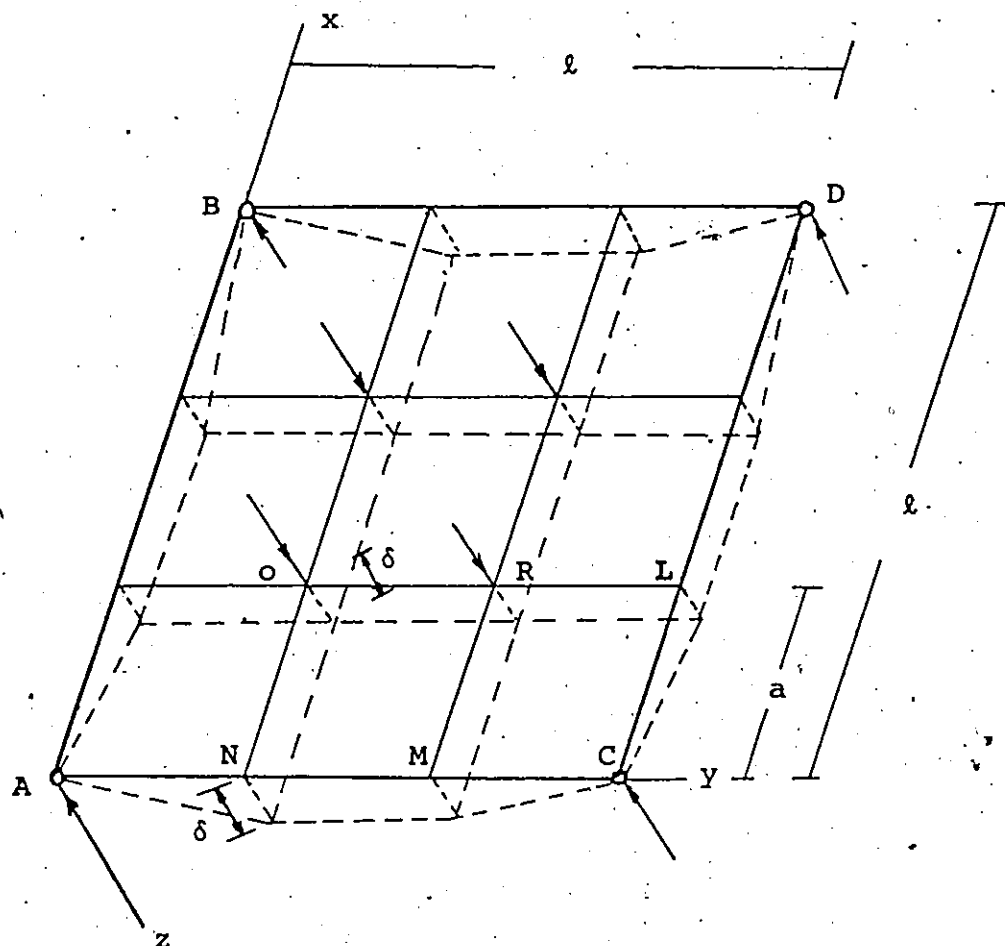


FIG. 3.5 COLLAPSE MODE ASSUMED FOR TEST TRUSS TYPE TWO (MODEL 2)

etric points as in Figs.(3.4) and (3.5) (Model 1 and Model 2).

3.2.2.1 Analysis of a first model

As seen in Fig. (3.4), the loaded points will drop down by a distance δ . It is assumed that the yield lines remain straight.

Considering the quarter surface MICS in Fig. (3.6), the change in the angle along the yielding line MS between the surfaces (MICS) and (RMSN) (see Fig. (3.4)) is given by:

$$\theta_A = \frac{\delta'}{a} = \frac{x\delta}{a^2}$$

Hence the energy dissipated at the yield line (SM) is given by:

$$E_{SM} = M_o \int_0^b \frac{x\delta}{a^2} dx = \frac{M_o \delta}{2} \frac{b^2}{a^2} \quad (3.14)$$

The total energy dissipated at the yield lines is:

$$E = 8E_{SM} = 4M_o \delta \left(\frac{b}{a}\right)^2 \quad (3.15)$$

The work done by the applied load is:

$$U = 4P \delta \quad (3.16)$$

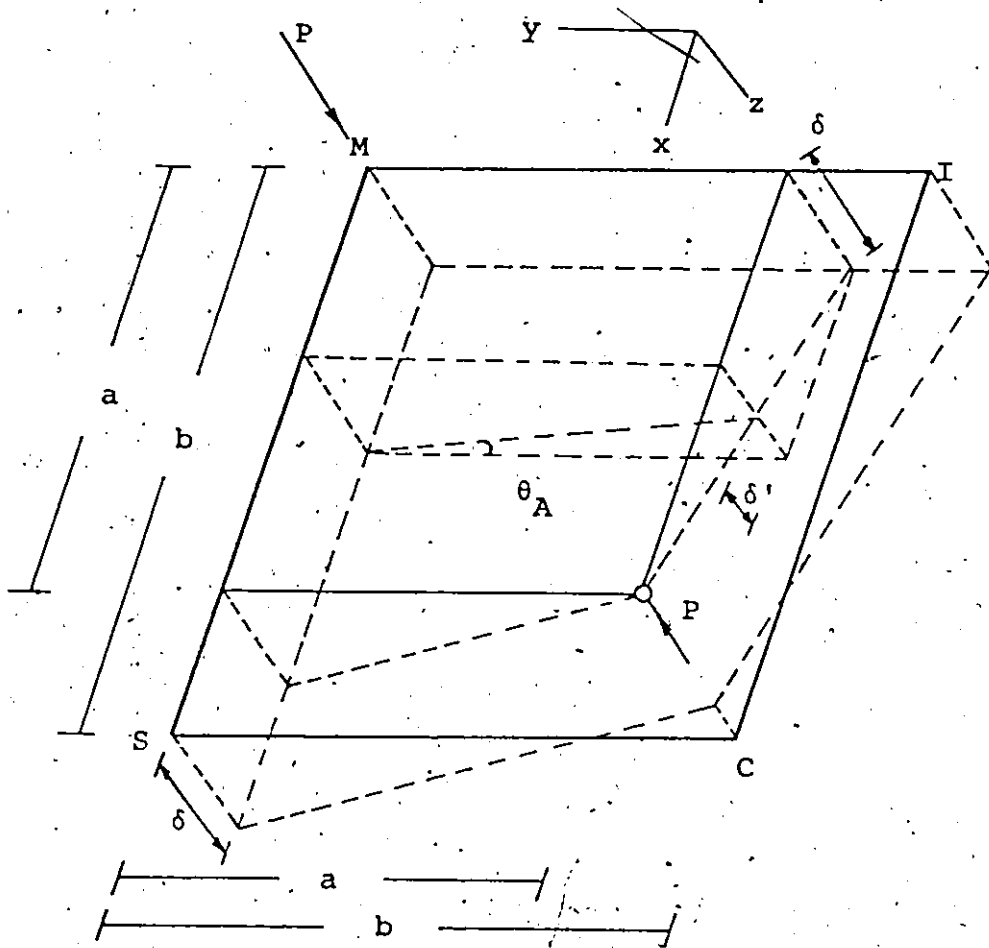


FIG. 3.6 ROTATION ANGLE ALONG THE YIELD LINES OF TYPE ONE MODEL

$$U = Q\delta \quad (3.17)$$

($Q = 4P$ the total applied load).

From equations (3.17) and (3.15):

$$U = E$$

or

$$M_0 \left(\frac{b}{a}\right)^2 = \frac{Q}{4} \quad (3.18)$$

3.2.2.2 Analysis of the second model

In (Fig. 3.5) the yield lines are illustrated and also the deformation of the truss under the ultimate load $4P$. For simplification again, consider the quarter of the truss as in (Fig. 3.7).

Along the yield line (RM) the change in angle between the surfaces (RLCM) and (ORMN), (see also Fig. 3.5), is θ_A , where the angle θ_A is given by the expression:

$$\theta_A = \frac{\delta'}{a} = \frac{\delta x}{a^2} \quad (3.19)$$

The energy dissipated at the yield line (RM) is:

$$E_{RM} = \int_0^a \frac{M_0 \delta x}{a^2} dx = \frac{M_0 \delta}{2} \quad (3.20)$$

The total energy dissipated at the yield lines is:

$$E = 8E_{RM} = 4M_0 \delta \quad (3.21)$$

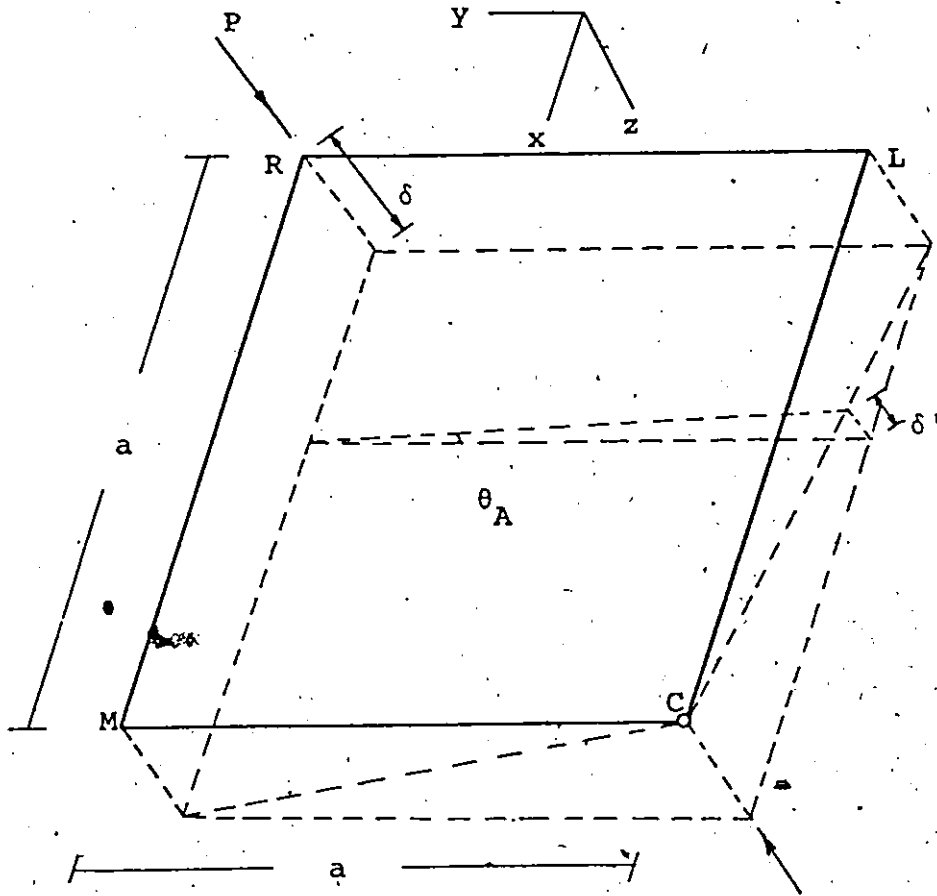


FIG. 3.7 ROTATION ANGLE ALONG THE YIELD LINES OF TYPE TWO MODEL

The work done by the external apply load is:

$$U = 4P \delta = Q\delta \quad (3.22)$$

(where $Q = 4P$ the total applied load).

From equations (3.21) and (3.22),

$$M_o = \frac{Q}{4} \quad (3.23)$$

3.2.3 Conflicts in the method treating the truss as a continuum

This simple energy method in some cases is in conflict with static considerations.

Let us consider the case in which an orthogonal grid space truss as in Fig. 3.8, is supported at the four extreme corners and loaded uniformly to collapse.

As in the previous cases, an expression can be derived which correlates the total applied load on the structure with the plastic moment per unit length M_o .

The expression which comes out is:

$$Q = \frac{16}{3} M_o \quad (3.24)$$

By considering now the equilibrium of the surface GIEF as in Fig. 3.9, we obtain:

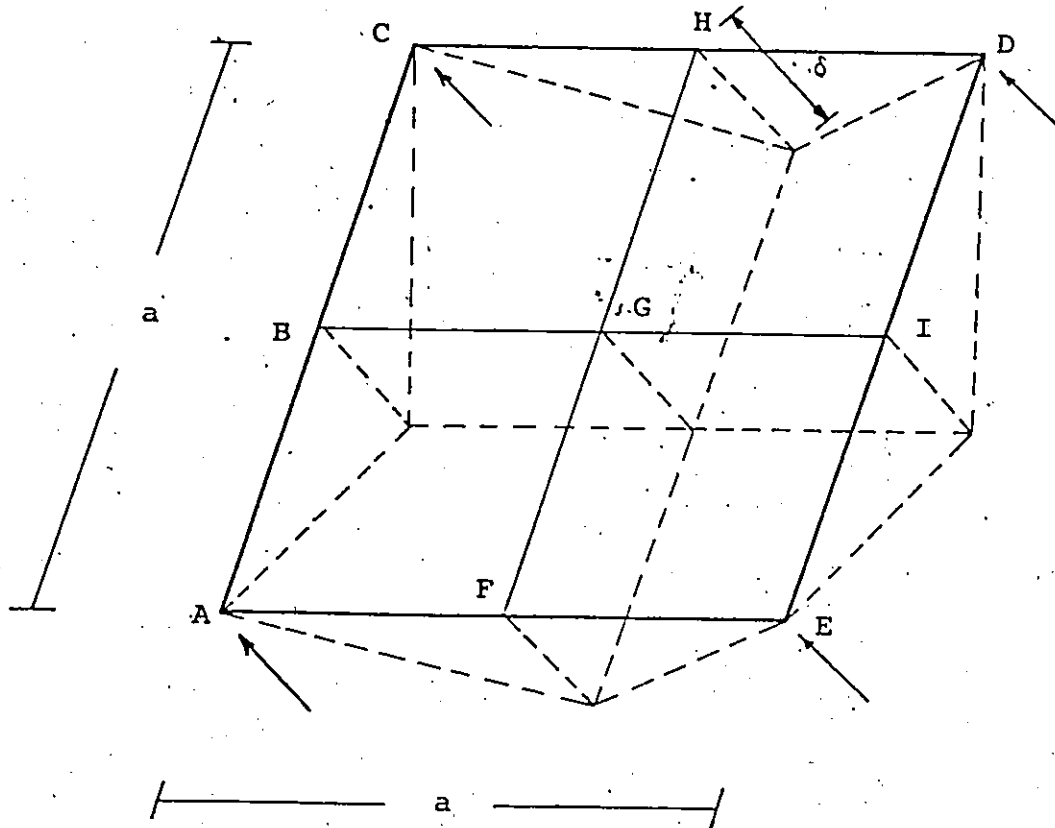


FIG. 3.8 COLLAPSE MECHANISM FOR ORTHOGONAL GRID TRUSS, SUPPORTED AT THE CORNERS AND UNIFORMLY LOADED

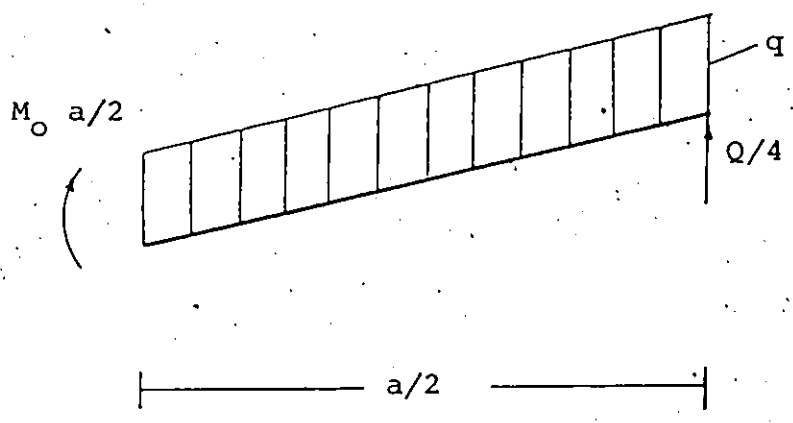


FIG. 3.9 FORCES AND MOMENTS ACTING IN A QUARTER OF THE TRUSS IN FIG. 3.8 IN COLLAPSE STATE

$$\frac{Q}{4} \cdot \frac{a}{4} = M_0 \frac{a}{2} + \frac{Q}{M_0} = 8 \quad (3.25)$$

Normally the solution which is based on kinematically admissible collapse modes is an upper bound of the solution, while the static equilibrium is a lower bound. Our analysis gives opposite results.

To resolve this conflict requires that there be in the centre of the truss, a negative moment as in Fig.3.10.

Considering that the positive plastic moment is in a length $K\frac{a}{2}$ (where K is a factor smaller than unity) the negative moment will be in a length $(1-K)\frac{a}{2}$.

Considering now the static equilibrium of the quarter of the truss as before and assuming that the negative moment is equal to M_0 , gives:

$$\frac{Q}{4} \cdot \frac{a}{4} = M_0 \cdot K\frac{a}{2} - M_0(1-K)\frac{a}{2} \quad (3.26)$$

$$\therefore M_0(2K-1) = \frac{Q}{8} \quad (3.27)$$

The ratio Q/M_0 must be less than $16/3$, which the energy method gives.

The ultimate computer analysis which follows in this text and which takes into account static equilibrium, gives

$$\frac{Q}{M_0} = 5.05$$

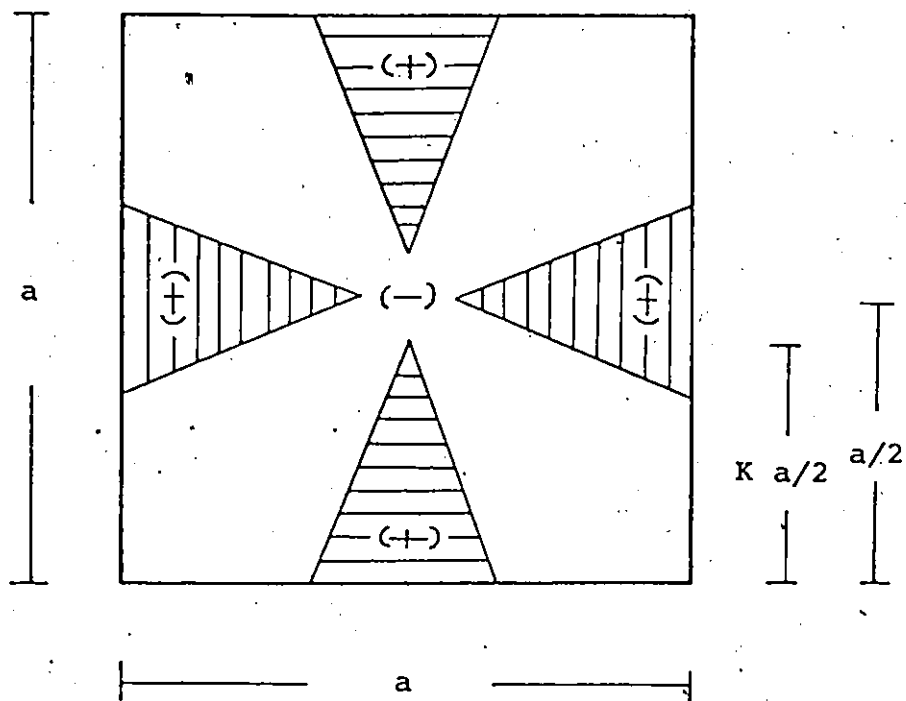


FIG. 3.10 ASSUMED YIELD ZONES FOR COLLAPSE STATE TO SATISFY STATIC EQUILIBRIUM

for a 10' x 10' truss supported at the four corners and uniformly loaded.

From equation (3.27) for $Q/M_0 = 5.05$:

$$\kappa = \frac{13}{16}$$

3.3 COMPUTER ANALYSIS

The ultimate-plastic analysis by computer, is actually a series of elastic analyses using the stiffness method. The basic assumption of this analysis is that of ideal elastic-plastic behaviour of the material, as explained in the introduction of this Chapter. Accordingly tension and compression members, after yielding and buckling respectively, are assumed to undergo sufficient amount of axial deformation while the force in the member remains constant, which permits redistribution of forces in the unyielded members.

The procedure followed by the computer programme, is similar to that used by Shin Be [2].

- (1) The co-ordinates of the nodes, the member numbering, the constraints, the member areas, and capacities in tension and compression (P_t, P_c) are specified.
- (2) A unit load is applied and the forces in all members computed (P_1), using the stiffness method. Until this step, the procedure is a simple elastic

analysis of an indeterminate space truss.

- (3) The capacity of each member (P_t or P_c) is divided by the force in the member due to unit load (P_1), (tension or compression respectively), and the lowest such ratio, K_1 , is found.
- (4) All member loads are multiplied by the ratio K_1 , and the force (K_1P_1) for each member is subtracted from the member capacity.
- (5) Those members for which the operation (4) leaves zero capacity, are removed from the structure.
- (6) The residual capacities in all the members ($P_t - K_1P_1$) or ($P_c - K_1P_1$), replace P_t and P_c .
- (7) The modified structure is then re-analyzed for unit load. The steps:(2) to (6) are repeated, obtaining another value of K , leading to the removal of a further member or members whose capacity is exhausted. This procedure continues until a sufficient number of members have been removed to allow the structure to collapse. The ultimate load for the frame is then ΣK .

Actually, by considering in each loop of the programme the residual capacities of the members which have not yet reached their ultimate capacity, we do not change the initial structure, but make use of the assumption

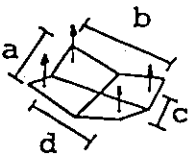
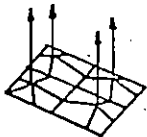
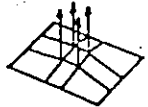
that the members which reach the ultimate capacity can carry this maximum load until a sufficient number of members yield so that the structure becomes unstable.

It must be mentioned at this point, that the whole procedure considers the connection of the bars at their ends by ideal pin-joints. In practice, such connections can never be realized and the rigidity of a practical type of connection will induce secondary stresses. However, in most practical cases, the presence of such secondary stresses does not influence considerably, calculated axial forces in the members.

In Table 3.1, the limit loads for orthogonal grids are compared accordingly to simple energy methods and ultimate computer analysis.

TABLE 3.1

COMPARISON OF CONTINUUM ANALYSIS AND
COMPUTER SOLUTION FOR ORTHOGONAL GRID
SPACE TRUSSES SUPPORTED AT FOUR POINTS
AND UNIFORMLY LOADED

Case	Q/M_0	
	Simplified Theory	Computer Calculated
 $c/a > 0.615$	$\frac{8\left(\frac{b}{a} + \frac{a}{b}\right)}{4\left(\frac{cd}{ab} - 1\right)}$ For $a = b = c = d$ $Q/M_0 = 5.33$	5.05
 $0.42 < c/a < 0.615$	$\frac{8}{3} \left[\frac{a(2b-d)}{d(b-d)} + \frac{b(2d-c)}{c(d-c)} \right]$ For $a = b, c = d$ $c/a = 0.6$ $Q/M_0 = 31.2$	37.0
 $c/a < 0.53$	$8 \left[\frac{d(2b-d)}{d(b-d)} + \frac{b(2d-c)}{c(d-c)} \right]$ For $a = b, c = d$ $c/a = 0.4$ $Q/M_0 = 18.3$	20.7

CHAPTER IV
CHORD BEHAVIOUR

CHAPTER IV

CHORD BEHAVIOUR

It is now appropriate to consider whether the behaviour of the chords allows a limit moment to be maintained under increasing rotation, which was considered in the assumptions and used in the analysis of the truss. Compression members that reach their ultimate load capacities in the inelastic range have load-deformation curves as in Fig. 4.1. Curve a) refers to the behaviour of long compression members, while (b) and (c) curves refer to intermediate and short compression members respectively, with the same axial and flexural rigidities.

The drooping characteristics of these curves are caused by inelastic buckling, and the "plateau" assumed in load-change of length relationship occurs for a reasonable range of deformation only for a short or very long compression members, and that in general, it cannot be considered to approximate to the rigid/plastic behaviour assumed in ultimate analysis.

By using a value significantly below the maximum capacity, a safe design is possible but a rational choice of such a value is difficult to make.

For purposes of illustration an ideal relationship between axial load and shortening can be derived.

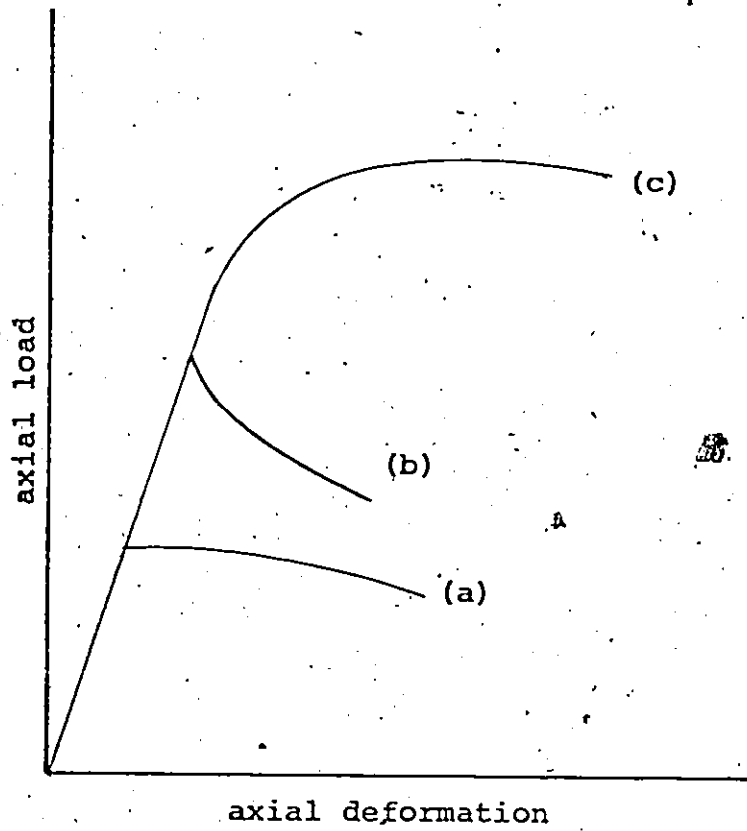


FIG. 4.1 TYPICAL LOAD-SHORTENING RELATIONSHIPS FOR STRUTS

The axial load is limited either by buckling, or by reaching the yield stress at the centre:

$$P = \pi^2 EI/L^2 = \sigma_e A \quad (4.1)$$

$$P(1/A + \Delta c/I) = \sigma_y \quad (4.2)$$

where A = cross-section of the bar

c = distance from C.G. to extreme fibre

I = moment of inertia

Δ = central bow in a strut

From the relation (4.2) we obtain:

$$\left(\frac{\Delta}{r}\right) = \left[\left(\frac{\sigma_y}{\sigma}\right) - 1\right] \left(\frac{r}{c}\right) \quad (4.3)$$

where r = radius of gyration

σ = mean axial stress

The average axial strain, is given by:

$$\epsilon = \delta/L = \sigma/E + \frac{\pi^2 \Delta^2}{4L^2} \quad (4.4)$$

where δ = axial deformation

L = the length of the bar

From (4.4), we obtain:

$$\epsilon E = \sigma + \left(\frac{\sigma_e}{4}\right) \left(\frac{\Delta}{r}\right)^2 \quad (4.5)$$

Using (Δ/r) from equation (4.3) and assuming that (r/c) is approximately 1, expression (4.5) becomes:

$$\epsilon(E/\sigma_Y) = \sigma/\sigma_Y + (\sigma_e/4\sigma_Y)(\sigma_Y/\sigma - 1)^2 \quad (4.6)$$

On the other hand, a fully plastic state for a bowed strut, neglecting plastic axial shortening, may be expressed approximately by:

$$\left(\frac{\sigma}{\sigma_Y}\right)^2 + \frac{\sigma}{\sigma_Y} \frac{A\Delta}{Z} = 1 \quad (4.7)$$

(Z = plastic section modulus)

By approximating $Z/A = r$, expression (4.7) gives:

$$\frac{\Delta}{r} = \frac{\sigma_Y}{\sigma} - \frac{\sigma}{\sigma_Y} \quad (4.8)$$

From expressions (4.5) and (4.8), we obtain:

$$\epsilon(E/\sigma_Y) = \sigma/\sigma_Y + \sigma_e/4\sigma_Y(\sigma_Y/\sigma - \sigma/\sigma_Y)^2 \quad (4.9)$$

The relations (4.6) and (4.9) have been plotted in Fig. 4.2. The dotted lines represent the relation (4.9), which was derived on the base of the fully plastic behaviour of the cross-section, for the same values of σ_e/σ_Y .

By considering the curves from the relations (4.6) and (4.9) for a certain value of σ_e/σ_Y , an envelope is obtained in which, ideally, must fit the load-shortening curve of every strut of the same σ_e/σ_Y .

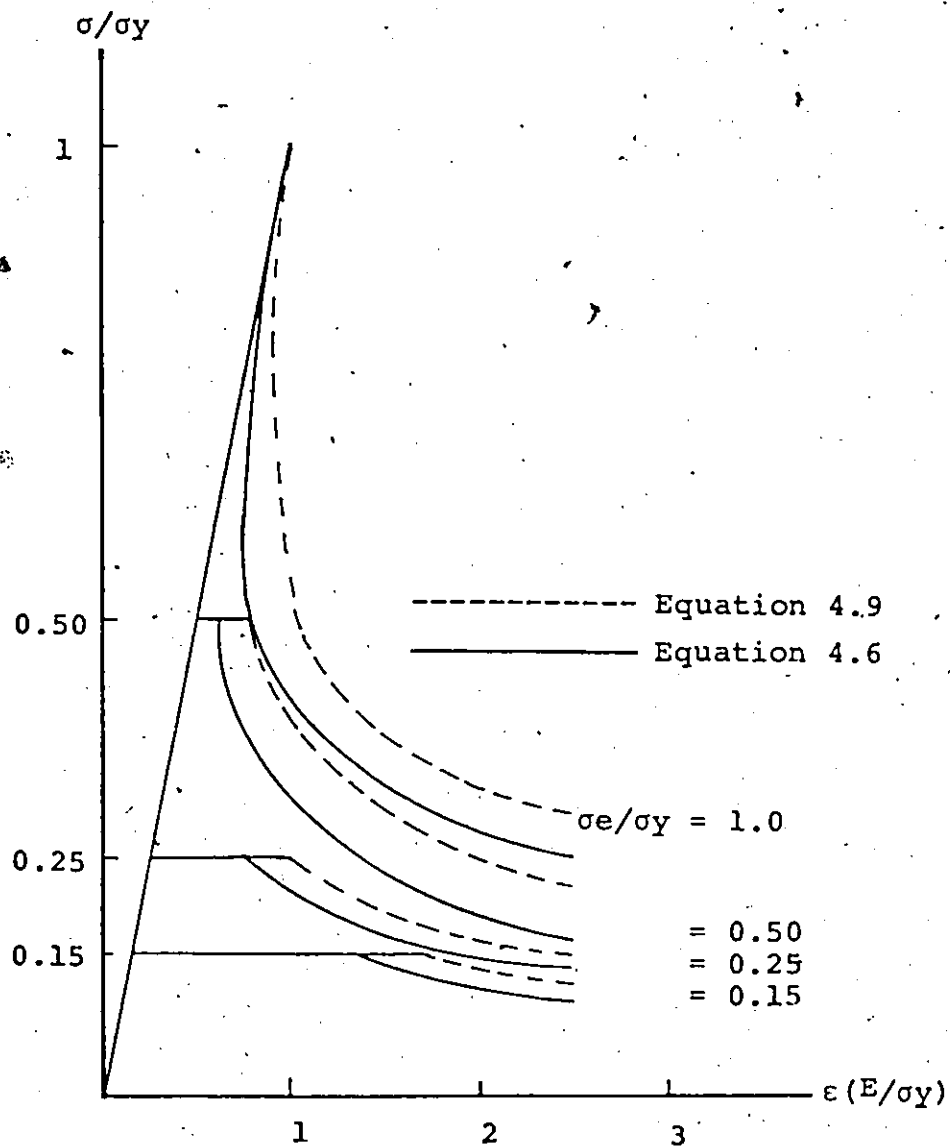


FIG. 4.2 IDEAL LOAD/SHORTENING RELATIONSHIPS FOR STRUTS

Unfortunately, the above expressions are not able to describe the post-buckling behaviour of the struts in order to use it in an ultimate analysis of a truss.

The foregoing derivations are essentially qualitative in nature to indicate the behaviour which, in practice, will vary with the shape of the cross-section.

For illustration purposes in Fig. 4.3, we can see the comparison of experimentally obtained curves which are compared with the theoretical curves according to expressions (4.6) and (4.9).

The behaviour of metal tension members is not expected to be more favourable since they fail at the points where the holes for connection purposes exist.

Tension members are not able to carry any load after reaching their maximum capacity, but will approach that capacity in a non-linear manner.

The ideal behaviour in Fig. 4.4, is assumed, with a limited post yield zone. In practice, compression members fail first and tension behaviour is of secondary interest.

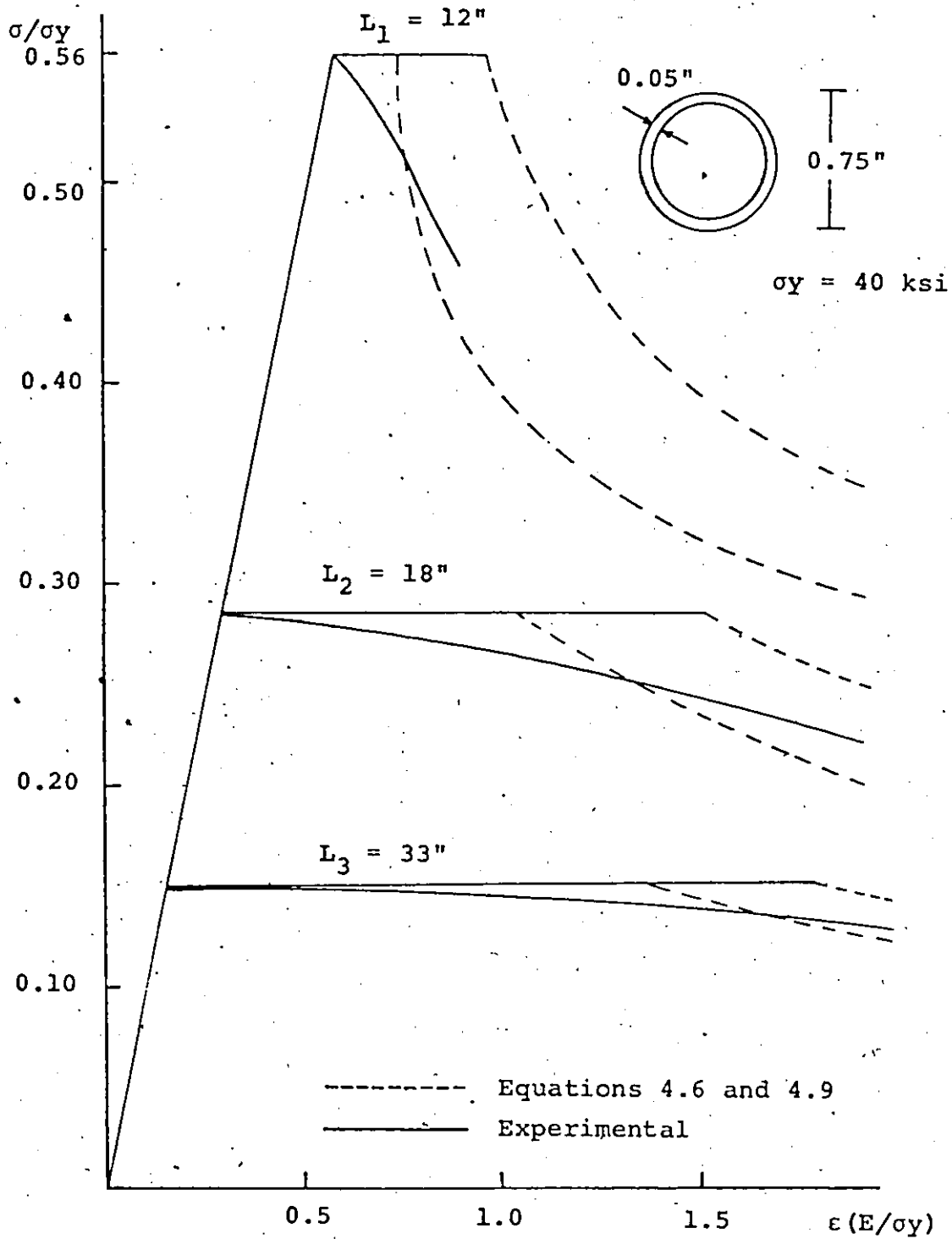


FIG. 4.3 COMPARISON BETWEEN IDEAL LOAD/SHORTENING RELATIONSHIPS FOR STRUTS AND EXPERIMENTAL RESULTS

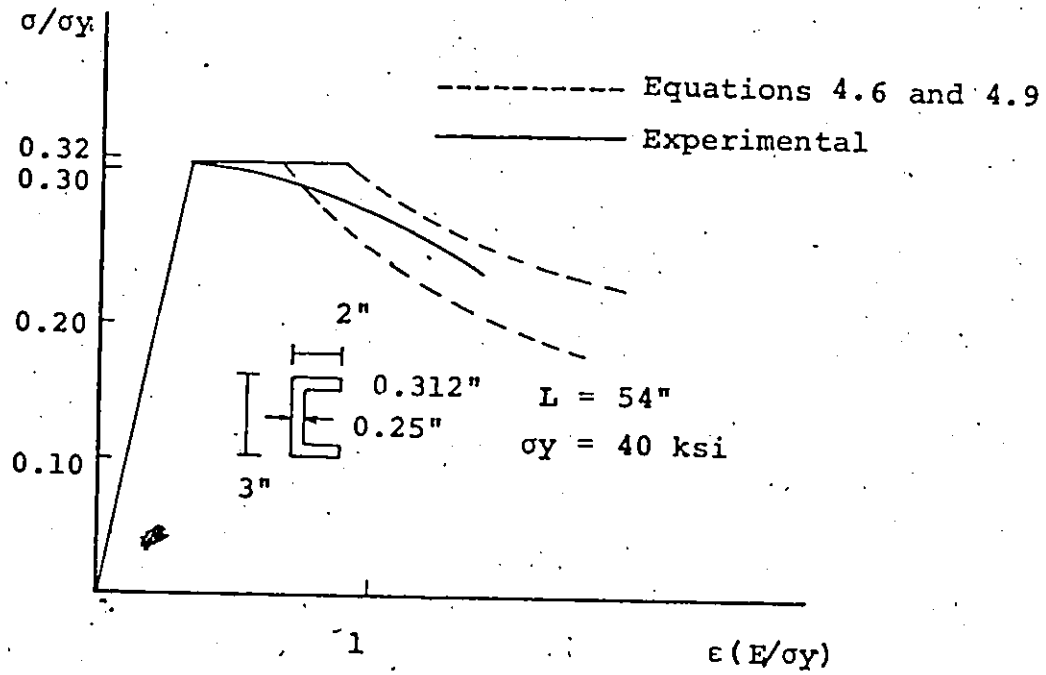


FIG. 4.3 COMPARISON BETWEEN IDEAL LOAD/SHORTENING RELATIONSHIPS FOR STRUTS AND EXPERIMENTAL RESULTS

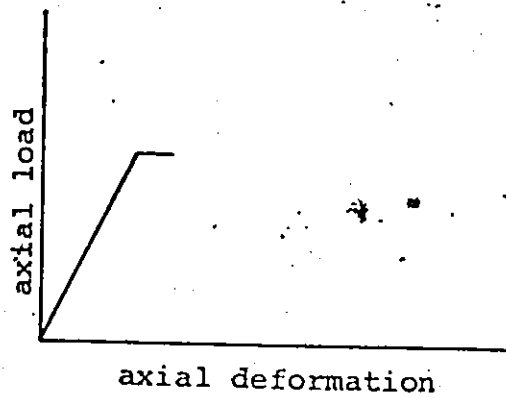


FIG. 4.4 IDEAL LOAD/AXIAL DEFORMATION CURVE FOR TENSION MEMBERS

CHAPTER V

TEST MODELS OF ORTHOGONAL SPACE TRUSSES

CHAPTER V

TEST MODELS OF ORTHOGONAL SPACE TRUSSES

5.1 INTRODUCTION

In order to determine the actual behavior of an orthogonal space truss, subjected to ultimate load, and to compare the theoretical considerations, a number of experiments have been carried out at the laboratories of the Civil Engineering Department at Concordia University. The trusses which have been tested were constructed with identical top and bottom chords and diagonals, respectively. The theoretical idea of replacing a discrete system with an equivalent continuum which was applied in simple energy analysis, is in agreement with this kind of structure. In addition, as we have already mentioned, the study deals with trusses of maximum possible identical parts (in order to minimize the cost) and also, under this condition, the ultimate load consideration is much more meaningful.

The models which have been tested are simple space trusses called M-DEC, used for a variety of roof types up to 164' span.

The main feature of the M-DEC system is the absence of nodal joint pieces. (Fig. 5.1).

Because the chords are continuous, the transfer of load into and out of each node is avoided, and only in a few

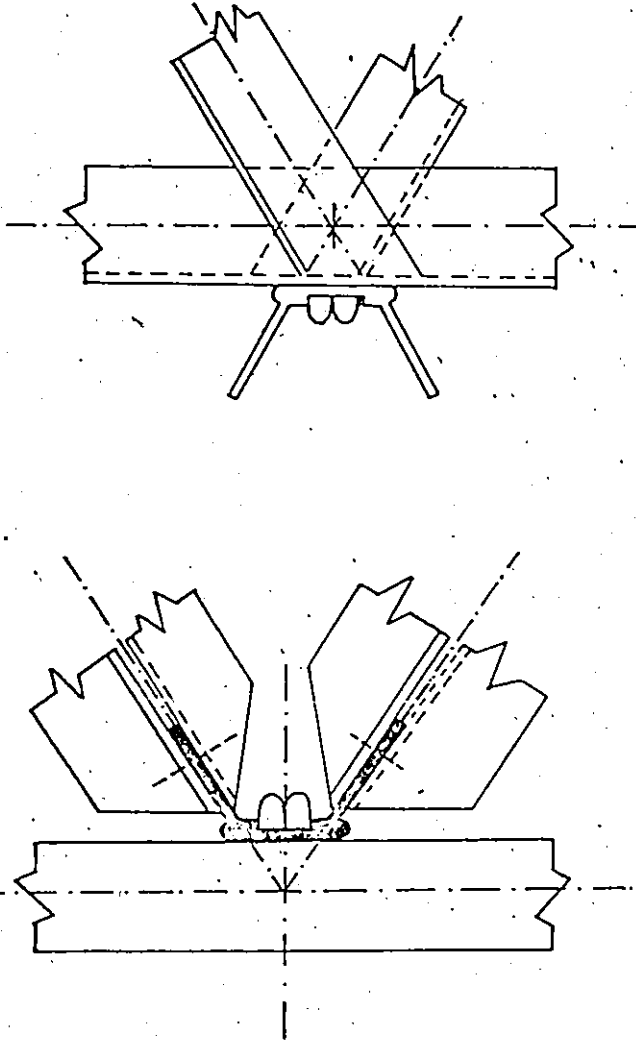


FIG. 5.1 DETAILS OF M-DEC SYSTEM

locations are more than three bolts for each node required.

5.1.1 Description of the Test Trusses

The test trusses are composed of two kinds of identical members, the top and bottom chords and the diagonals. The material from which all the members are made is the aluminum alloy 6351-T6, a material, the behaviour of which approaches in a tensile test, the idealized form of elastoplastic behaviour.

In Fig. 5.2 are illustrated the cross-sections of the chord and diagonal members which have been used for the test models.

Structural arrangements as shown in Figs. 5.3, 5.4 and 5.5, have been examined.

The continuous lines represent the top-chords and the dotted lines, the bottom chords and the diagonals.

Point "A" is one of the four supports of the trusses, while Point "B" is one of the four points at which the load is applied.

Fig. 5.4 shows a similar truss to that of Fig. 5.3 with the support at the end of the truss, while Fig. 5.5 illustrates an identical truss to that of Fig. 5.4, but with a smaller span.

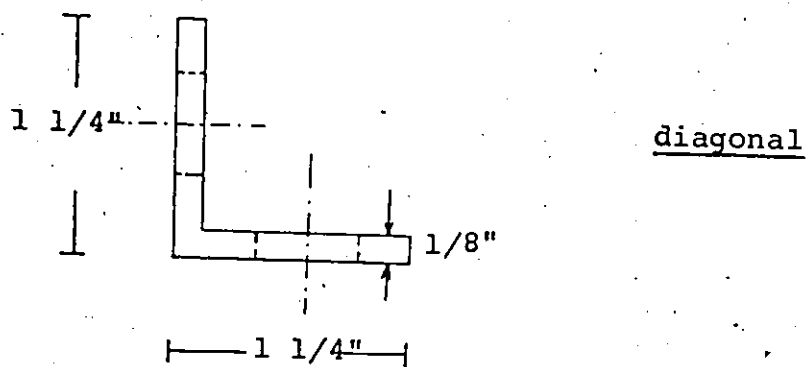
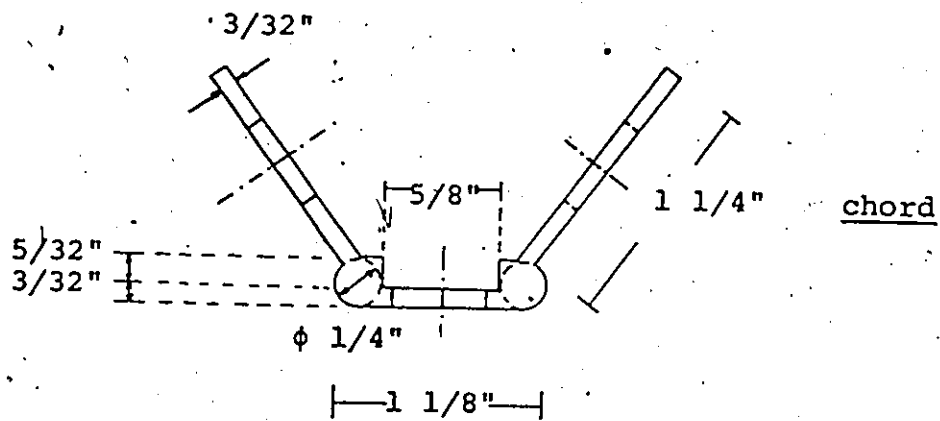


FIG. 5.2 CROSS-SECTIONS OF CHORDS AND DIAGONALS
USED FOR THE TEST TRUSSES

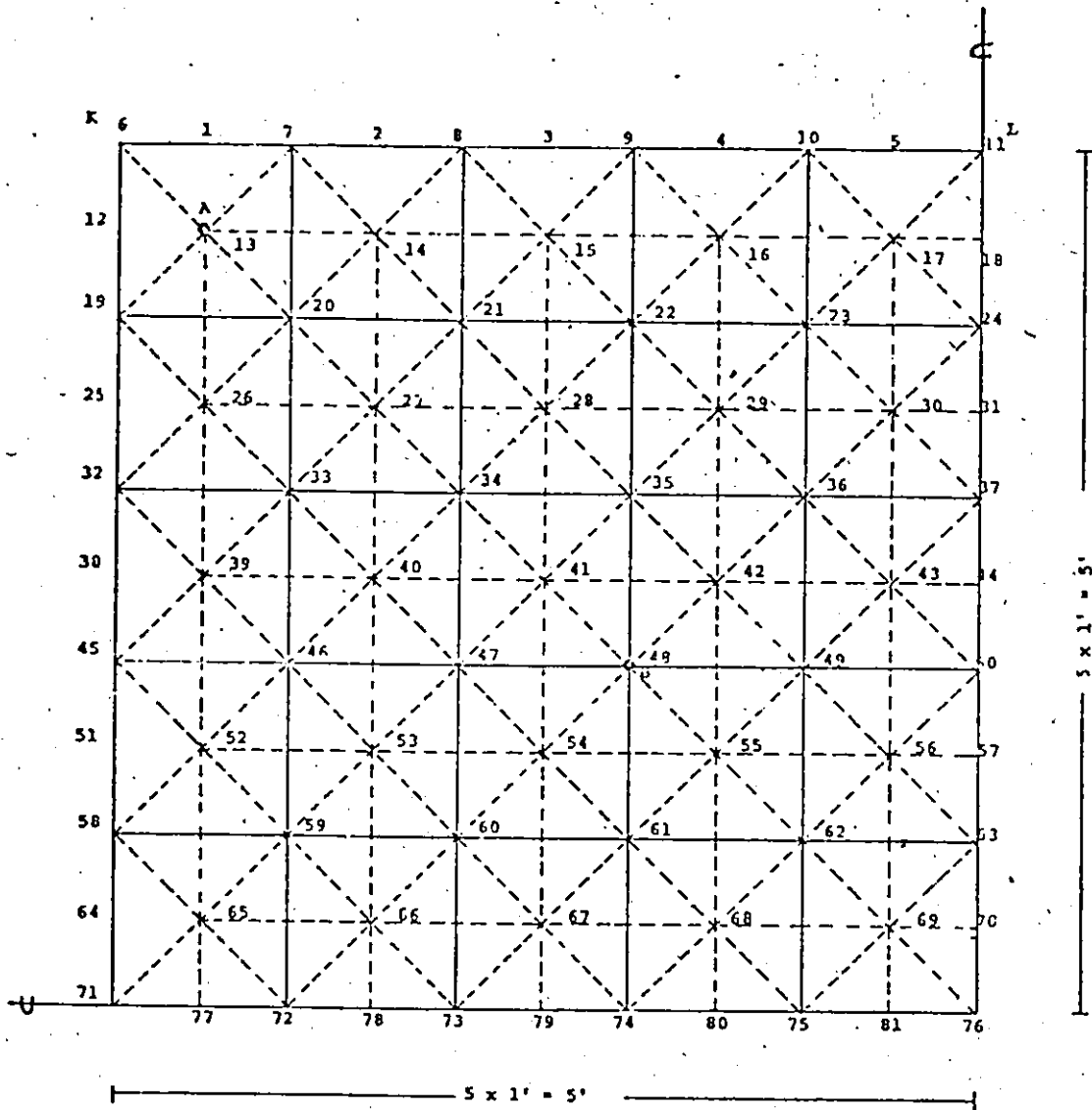


FIG. 5.3 FIRST TEST MODEL, SUPPORTED AT A AND LOADED AT B. (QUARTER OF THE SURFACE). DEPTH OF THE GRID 9.5"

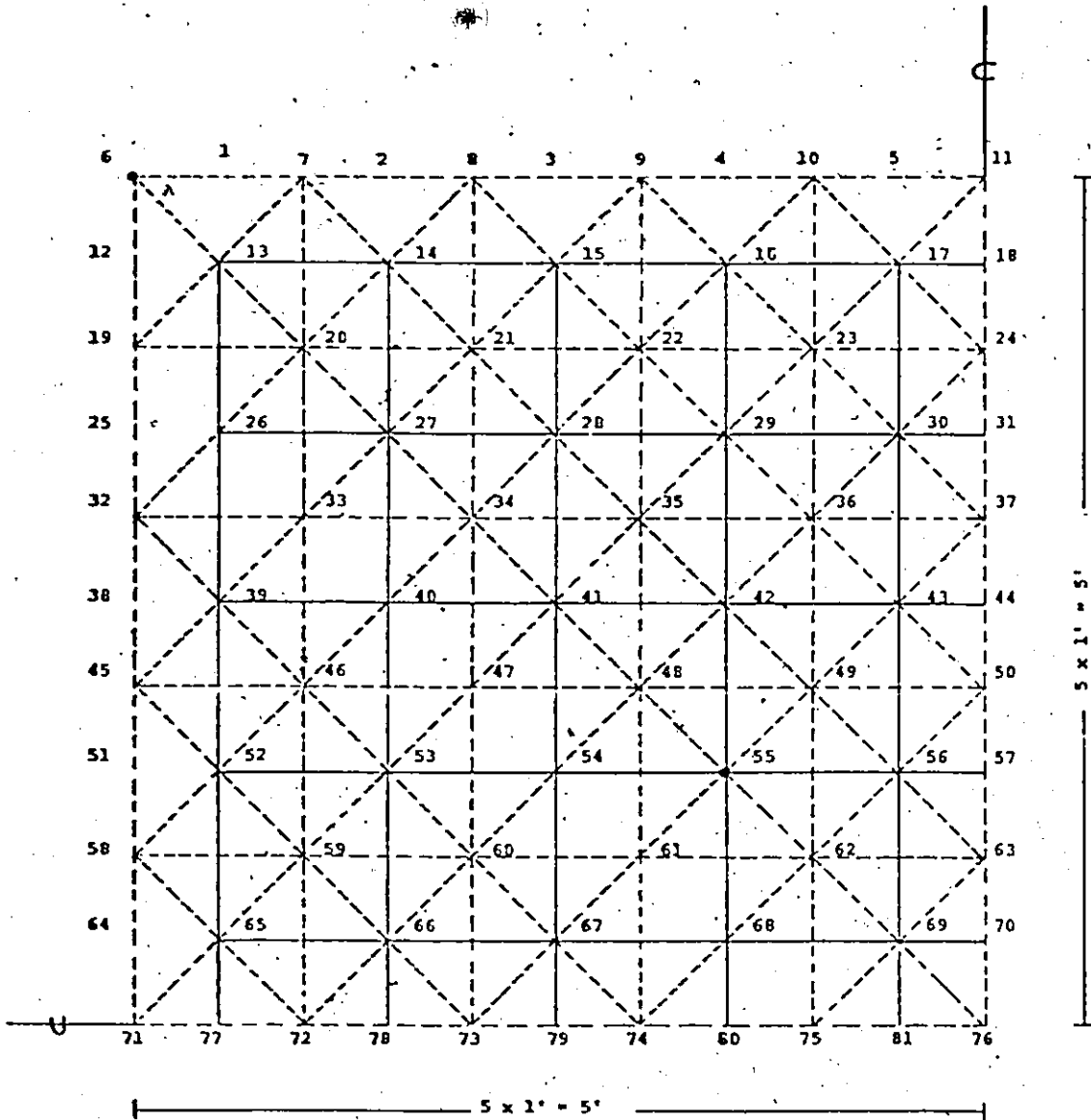


FIG. 5.4 SECOND TEST MODEL SUPPORTED AT A AND LOADED AT B. (QUARTER OF THE SURFACE). DEPTH OF THE GRID 9.5"

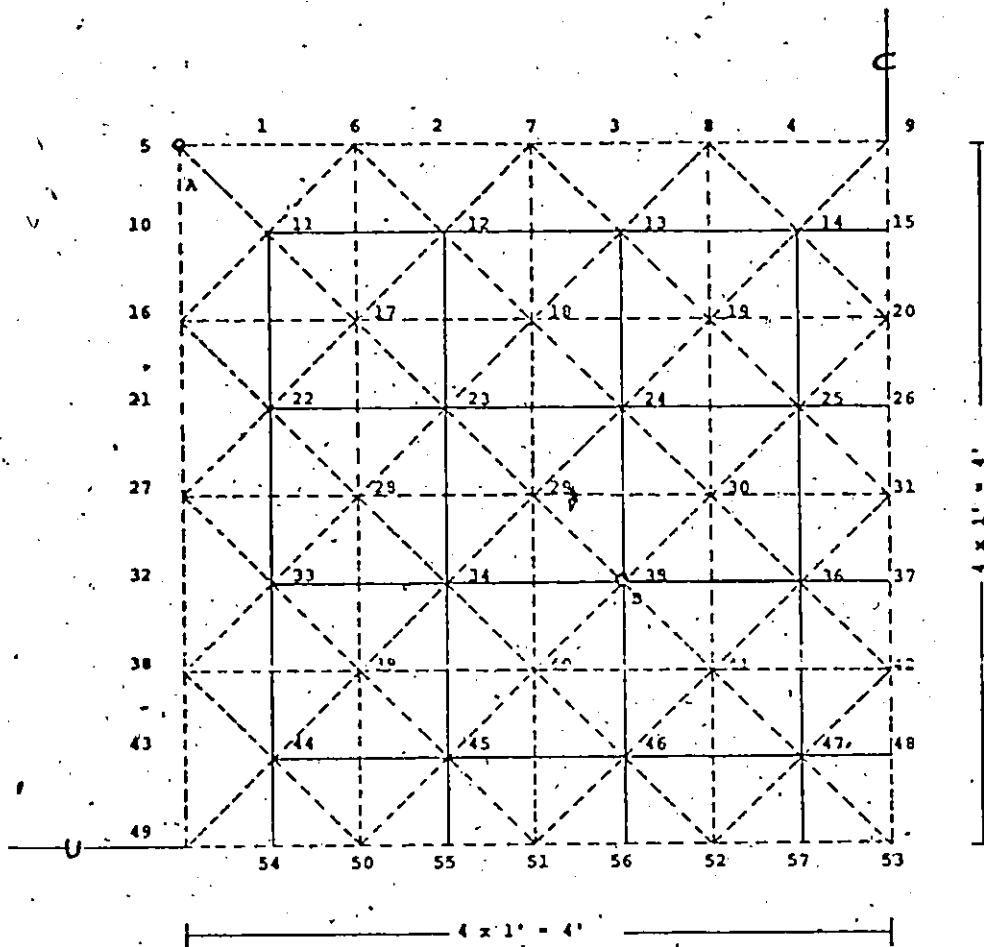


FIG. 5.5 THIRD TEST MODEL LOADED AT B AND SUPPORTED AT A.
(QUARTER OF THE SURFACE). DEPTH OF GRID 9.5"

In all the trusses which have been examined, the chords and the diagonals were identical, respectively, as illustrated in Fig. 5.2. The chords were continuous and the same load procedure has been applied for all the test trusses.

The reinforcing of some diagonals was required to ensure failure according to theoretical considerations, as will later be explained in this text.

The capacities P_t and P_c in tension and compression, respectively, of the members which have composed the test models, are illustrated in Table 5.1.

The No. 3 and No. 4 members (diagonals) have been used as reinforcing members at particular locations.

The limit compression capacity of the chords for a length 12 inches (since the chords form square grids 12 in. by 12 in.) is governed by failure in torsion, while the capacities of the diagonals are governed either by bolt failure, or by bearing failure.

5.2 THEORETICAL ANALYSIS OF THE TEST MODELS

A theoretical analysis of the test models, according to simple energy and computer analysis methods, is required in order to compare experimental and theoretical results.

5.2.1 Analysis According to Simple Energy Method

The truss model which has been illustrated in Fig. 5.3

TABLE 5.1

TENSION AND COMPRESSION CAPACITIES OF THE
MEMBERS USED IN THE TEST MODELS

No.	Member Description	P_t (kip)	P_c (kip)
1	Top and bottom continuous chords which form square grids 12" x 12"	11.000	6.500
2	Simple diagonal which is connected to the chords with one bolt 3/8" dia.	3.000	4.300
3	Double diagonal which is connected to the chords with one bolt 3/8" dia.	4.300	4.300
4	Double diagonal which is connected to the chords with two bolts 3/8" dia.	6.000	9.000

has been analyzed in sub-section 3.2.2.1, in general form. The expression which came out of the analysis was:

$$M_o \left(\frac{b}{a}\right)^2 = Q/4 \quad (5.1)$$

By referring to Fig. 5.3, and Fig. 3.4, we can verify that for this model, the values of a and b are 30 in. and 36 in., respectively. However, the expression (5.1) resulted from an ideal analysis which examined a continuous and uniform system instead of a discrete system, and this uniformity assumes that the end chords (i.e., KL chord at Fig. 5.3) are half of the capacity of the central identical chords. Because the model is composed of identical chords, due to this additional cross-section of the end-chords, an additional plastic moment is obtained. By referring again to Fig. 3.6, the energy dissipated at the yield lines MS' and MI', is given by

$$E = \left[\frac{M_o \delta}{2} \left(\frac{b}{a}\right)^2 + M_o \frac{(b-a)b}{2a^2} \delta \right] 2 \quad (5.2)$$

The work done by the external applied load at point M, is:

$$U = P\delta = \frac{Q}{4} \delta \quad (5.3)$$

From Eqs. (5.3) and (5.2), we obtain

$$M_o \left(\frac{b}{a}\right)^2 + M_o \frac{(b-a)b}{2a^2} 2 = \frac{Q}{4} \quad (5.4)$$

Using the values $b = 36$ in. and $a = 30$ in. which correspond to the test model gives:

$$\frac{Q}{M_o} = 6.72 \quad (5.5)$$

Remembering that M_o is the plastic moment per unit length which is given by the expression (3.1), and by using as ultimate compression strength for the chords $P_u = 6,500$ lbs. then $M_o = (6,500 \times 9.5) : 12 = 5,145$ lb/in/in., the total load which the structure can carry is $Q = 34,575$ lb.

The model trusses which have been illustrated in Fig. 5.4 and Fig. 5.5, have also been analyzed in general form, in sub-section 3.2.2, and the expression resulting was:

$$M_o = \frac{Q}{4} \quad (5.6)$$

Since the plastic moment per unit length in the models was $M_o = 5,145$ lb.in/in., the total load which these trusses could carry was $Q = 4 \times 5,145 = 20,580$ lbs.

5.2.2 Analysis of Test Models According to the Computer Method vs. the Energy Method

The assumptions made in the various steps of the method have been described in Section 3.3, in particular that the members which buckle can carry their maximum capacity while shortening sufficiently to permit the redistribution of forces.

The actual behaviour of struts has been shown to differ from this assumption.

Figure 5.6 illustrates a comparison of an experimentally obtained curve for a chord identical to those chords used in the models, with the theoretical curves according to expressions (4.6) and (4.9).

The chord illustrated was 12 in. in length. Failure was due to torsional instability.

As has already been mentioned, the capacities of the diagonals (Table 5.1) are governed either by bolt failure, or by bearing failure. The assumption that these members will elongate sufficiently to permit a redistribution of forces in the remaining members, may not be valid.

For this reason some diagonals were reinforced in order to ensure that they did not fail.

The reinforcement adopted for the diagonals was as shown in Fig. A.1.

The results of the analysis are represented in Fig. A.2.

The load for the first chord buckling was 30,431 lbs. (the elastic capacity of the structure), while the ultimate load reached on the 15th cycle of the analysis, according to the computer programme, was 40,418 lbs. Diagonals failed

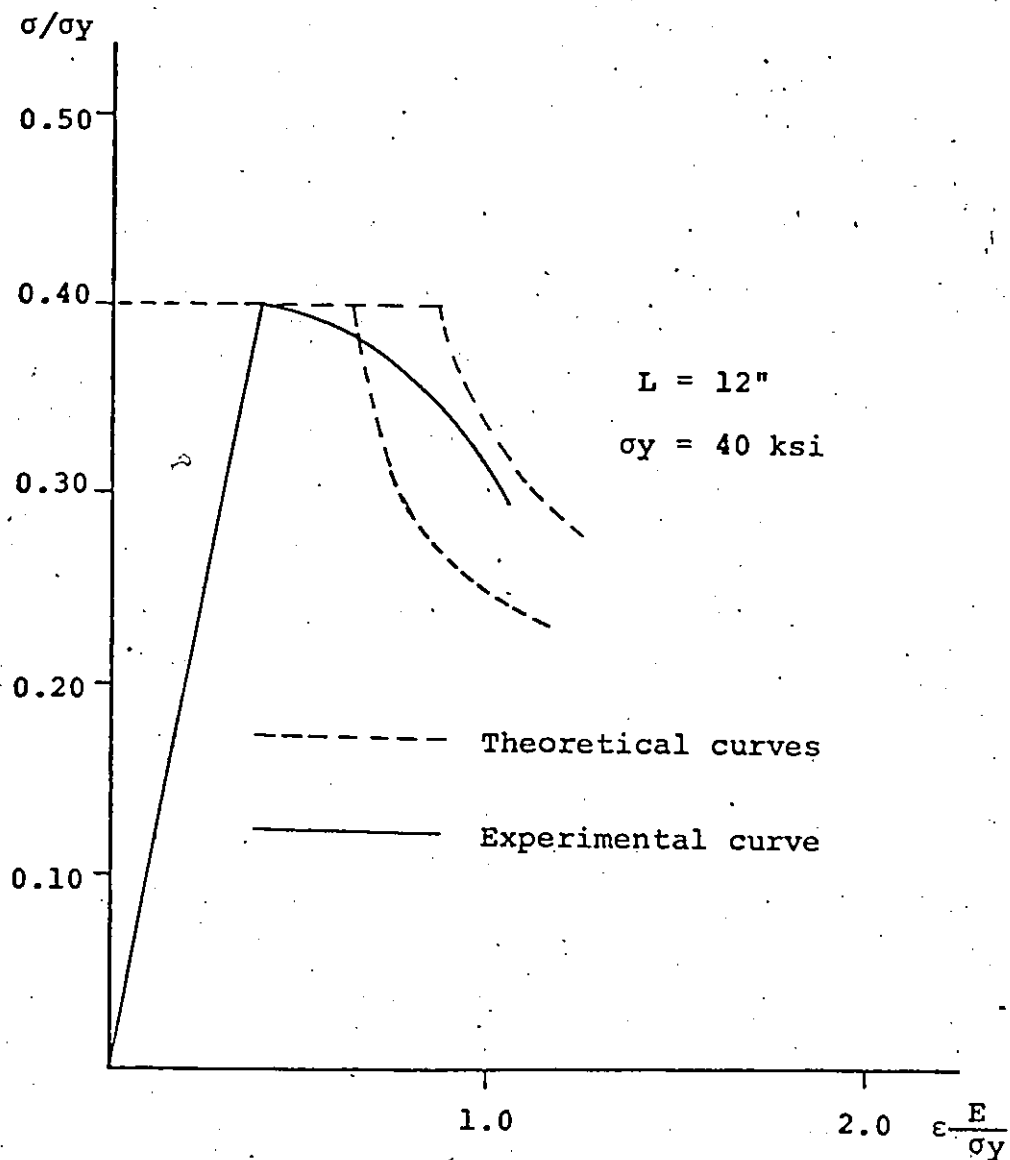


FIG. 5.6 COMPARISON BETWEEN IDEAL LOAD-SHORTENING RELATIONSHIPS FOR STRUTS AND EXPERIMENTAL RESULTS FOR A CHORD

in the 10th, 13th, 14th and 15th cycles, but the change in load from the 10th to the 15th cycle was only 900 lbs. in 40,400 lbs., and hence was negligible.

Flower et al[5] illustrates that "the truss forces are generally, relatively independent of the web rigidity, and hence the sequence of the chord failure will not be affected by the reinforced diagonals.

It is also seen that for this initial test, the simple energy analysis gave an ultimate load of 34,575 lbs., which is not far from the prediction of the computer analysis. The sequence of failure according to the computer analysis, also is similar to the assumption of the simple energy method.

The same procedure followed for the computer analysis of the trusses shown in Figs.5.4 and 5.5. A local reinforcement of several diagonals in these trusses was also required. The sequence of failure which was determined by the computer analysis for these trusses is illustrated in Figs.A.3 and A.4, respectively, as well as the values of loads for the first member failure (elastic capacity of the structures) and the ultimate capacity of the structure.

In the above figures, it is also seen that some diagonals fail in intermediate cycles, but since they fail far from the first cycle, the test models were considered satisfactory, in order to examine the behaviour of the trusses after their elastic capacity was reached.

It is seen from these figures, that the ultimate capacities given by the computer analysis for these trusses are approximately equal, to that given by the simple energy analysis. ($Q = 4M_0$, where M_0 is the same for these frames). The discrepancy between the two results is because some of the diagonals failed in intermediate cycles.

CHAPTER VI

CONDUCT OF THE TEST - TEST
RESULTS

CHAPTER VI

CONDUCT OF THE TEST - TEST RESULTS

6.1 TEST SET-UP

In Figures 5.3, 5.4 and 5.5, are illustrated the test models which have been used in order to compare experimental and theoretical results. All the test models, as we have already mentioned, were composed of identical chords and diagonals, respectively. Some diagonals were reinforced, as explained earlier.

In order to apply the load of four symmetrical points the arrangement illustrated in Fig. A.5 was adopted. The load was applied from the jack to the system of beams. The two beams which were in contact with the truss rested on steel blocks which were fitted inside the chords, so that the load was applied exactly at the joints. A similar arrangement was adopted for the support-joints, which were free to rotate without constraint.

6.2 INSTRUMENTATION6.2.1 Load Measurements

The load was applied through the jack, as in Fig. A.5. At each loading stage, readings were taken of the load, stress and deflection.

6.2.2 Deformation Measurements

The following measurements were taken.

- (1) The strains in the top-chord members along the yield lines. In Fig. A.6, the location of the strain gages for the first test model are illustrated. As shown in the picture, there were two strain-gages in each member, one on each flange located on the neutral axis of the cross-section at the mid-way point between the adjacent nodes.
- (2) The vertical deflections of some of the characteristic joints of the trusses, such as the central joint of the structure, the joint in which the external load was applied, the joints which determine the assumed yield lines, were measured by dial-gages.

6.3 TESTING PROCEDURE

The testing procedure followed was essentially the same for all the three test models, except for the difference in the load history. The load was increased at a steady rate to a convenient value and stopped for readings to be taken. Due to relaxation, loads dropped during the reading time, and hence, load readings were taken at the start and at the end of each load stage. All the three models tested monotonically to failure, and a sufficient

number of load stages were chosen to study the behaviour of the models completely.

6.4 TEST RESULTS

6.4.1 Model 1

The vertical deflections of joints 45, 71, 48, and 76, of this model (see Fig. 5.3) are illustrated in Table A.1. The experimentally obtained ultimate capacity of the truss was 31,908 lb greater than the elastic capacity which the computer analysis determined and less than the ultimate capacity which the computer analysis and simple energy method gave.

The failure of the truss is illustrated in Fig. A.7. Unfortunately, the failure of the truss occurred in a different manner from that given by the simple energy method and computer analysis. Until the stage in which the failure of the structure began, no visual buckling of members was observed, except for some top-chords close to the joints where the load was applied. These chords were starting to buckle when the total applied load was 14,727 lbs., in spite of the fact that the external load was applied exactly at the joints.

This local buckling may have occurred because of the concentrated loads.

Referring to Fig. 5.3, the top member 19-32 failed and the bottom member 26-39 also failed due to local bending caused by secondary deformation in tension. Also, it was observed that the triangle formed by the joints 6-13-19 remained without rotation up to failure.

In Table A.2, are listed, the strains given by the strain gages for the members along the yield (there were two strain-gages in each member). Column 4 gives the average strain for each member and column 5 gives the axial force for each member which corresponds to the strain. The strains are given in microinches/in., and Young's Modulus of Elasticity is 10^7 lb/in² for aluminum. Column 6 gives the forces in each member according to computer analysis for comparison.

In Figure A.8 are illustrated the forces in the members along the assumed yield lines of the first test model, for the total load in the structure 14,727 lbs., and 31,908 lbs. The curves (a) represent the forces according to the experiment, while the curves (b) the forces according to computer analysis. The discrepancy has not been fully explained.

In Figure A.9, the load deflection relationships for the joints 45, 71, 48, 76 are plotted according to computer analysis and experimental results, listed fully in Tables A.1, and A.3.

A second truss, identical to Model I was tested. The

results which resulted from the strain-gages and the deflections of the above joints were similar to those obtained in the first test, while the pattern of failure was identical to the first one.

6.4.2 Model 2

The second model was tested in the same manner. The experimental results are compared with the computer analysis in Figure A.10, for the load-deflection relationships for the joints 45, 71, 76, 55 (see Figure 5.4) according to Tables A.4 and A.5.

As can be seen from the above figure, the experimental ultimate load of the structure is bigger than the elastic capacity which the computer analysis determined, but again no buckling was observed in any member of the truss. The failure of the truss occurred because eccentricity in the top joint 13 occurred. In Fig. A.11 the failure of this joint is illustrated.

A second truss, identical to that of Model 2 was tested and similar load-deflection relationships were obtained, while the failure pattern and ultimate load were identical.

In both cases, the collapse load was bigger than the elastic capacity which the computer analysis determined, but no buckling was observed in any member, the failure of the structure being due to local failure.

6.4.3 Model 3

In order to eliminate the local failure which was observed in the previous test model, a special reinforcement made for the member 11-12, (see Figure 5.5) so that the resistance of this member was increased.

The failing load was, this time, 22,050 lbs., and much higher than the elastic capacity of the structure given in the computer analysis. The only member observed to buckle was the member 13-14 (see Figure 5.5), when the total applied load on the structure was 19,600 lbs. Finally, the structure collapsed when the member 5-16 failed in tension, due again to local failure.

In Figure A.12, the load deflection relationships for the joints 27, 49, 35, 53 of this third model are plotted according to computer analysis and experimental results, as given fully in Tables A.6 and A.7.

CHAPTER VII

DISCUSSION OF TEST RESULTS

CHAPTER VII

DISCUSSION OF TEST RESULTS

At the beginning of this Chapter, we must point out the following:

- (1) For the various models which have been tested, the relationship between the total applied load on the structure and the vertical deflection of some characteristic joints have been plotted in each case, as obtained from the computer analysis and the experimental results. The curves plotted according to the computer analysis are up to the point when a diagonal fails, because after this point, as explained earlier, there is no point in continuing the analysis through the computer programme.
- (2) In all the load-deflection graphs made for the various joints in each model, on the basis of experimental results, the self weight of the structure and the weight of the beams and jack were not considered. This load was approximately 800 lbs. If this load is added to the load-deflection curves plotted for the various joints, the experimental curves will be closer to the theoretical curves derived from the computer analysis, however, the difference is still considerable. Also, we have to recognize that the experimental ultimate capacity of the models was 800 lbs. more than the quoted value.

- (3) In all the models tested, in spite of the fact that they were simple square space trusses loaded symmetrically, the built-in imperfections and unavoidable variations in load intensity lead to one member reaching its capacity first, before others which carry, theoretically, identical loads because of their symmetry.

7.1 TEST 1

In the first test model, there was poor agreement between the experimental results and the theoretical predictions.

The ultimate capacity of the structure was higher than that predicted by the computer analysis for the elastic capacity of the truss. The failure mode was unexpected due to local failure.

Referring to Table A.2, according to strain-gage indications (for relatively high loads), the members (22-23), (23-24), (35-36), and (36-37) had higher axial forces than the computer analysis predicted, while the rest of the members had lower values. Also, these members carried loads in excess of the predicted (experimentally and theoretically) ultimate capacity when the total load on the structure exceeded 27,000 lbs. It is conjectured that the axial load on these compression members was applied with eccentricity, reducing the compression at the flange tips. This acts to

stabilize the member against torsional buckling.

Hence, these members carry more load than the torsional buckling predicts.

Also, because of the imperfections in the various joints of the truss, (diagonal-chord connections) which were unavoidable for this small depth of the truss, a rotation seemed to be produced at the joints. This joint rotation and also the slippage of the bolts, seems to be the reason for the differences in load-deflection curves.

7.2 TEST 2

The second test model behaved similarly. As is illustrated in Figure 5.4, the second test model was identical to the first one, except that the supports were at the extreme corners of the truss.

As the simple energy method predicted, the second model had half the ultimate capacity of the first one. A closer behaviour to the theoretical one was expected, since some of the secondary effects were eliminated because of the lower value of the ultimate load capacity. The structure failed under a load bigger than its elastic capacity but again, because of local failure, no buckling of any member occurred.

The differences at the load-deflection curves for the joints 45, 71, 76, and 55 between the computer analysis and

experimental results was also considered to be due to joint rotation and bolt slippage.

7.3 TEST 3

The third test model, the same type as the second one, with a different span, also had the same ultimate capacity, theoretically. Because of the elimination of the secondary effects which caused failure of the second model, the structure failed, this time, under a load 22,050 lbs., compared to 23,900 lbs. predicted from the computer analysis, again, because of local failure. The member (13-14) (see Fig. 5.4), buckled at 19,600 lbs.

The reason for the differences in the load deflection curves between the computer analysis and the experimental results for the joints 35, 53, 49, 27 are again as in the previous cases.

From all the models tested, a redistribution of forces seems to have occurred because of the bolt slippage, so that the trusses could carry more load than their predicted elastic capacity from the computer analysis, without buckling of a member.

However, that the members (22-23) and (23-24) of the first truss model, according to the strain-gage indications, carried load more than their predicted capacity, could also explain the higher load obtained without any chord buckling.

In the third test model, in which some secondary effects had been reduced so that the frame could carry a high load, the buckling of the (13-14) member was observed (see Fig. 5.4), but under a load 19,600 lb. i.e., more than the elastic capacity of the structure. According to computer analysis, this member would buckle in the second cycle.

CHAPTER VIII
CONCLUSIONS

CHAPTER VIII

CONCLUSIONS

Three truss models were tested to investigate the ultimate strength of orthogonal grid space trusses. All the truss models were tested monotonically until failure. The experimental total load in the structure-vertical deflection curves of some characteristic joints are compared with the corresponding curves from computer analysis. The basic assumption which the computer programme used was that the struts buckling have a "plateau" in the load-change of length relationship of sufficient extent to permit a redistribution of the moments.

Predictions based on the simple energy analysis are compared to computer solutions and their experimental results.

The assumptions of the load/shortening relationship of struts also are examined.

The following conclusions are attained:

- (1) A rapid approximation for the collapse load for flexural failure of orthogonal grid flat space trusses composed of uniform members based on simple energy analysis has been shown to be reasonably valid when compared to the computer solutions and seems to be not far from the experimental results.
- (2) The load/shortening relationship for struts cannot

be considered to approximate the rigid/plastic behaviour assumed in the ultimate load analysis and the force which a member can carry after buckling, for an ultimate analysis of orthogonal grid space trusses, is a matter for further study.

- (3) The failure mode assumed for the simple energy method is similar to that of the computer analysis. However, the computer analysis indicates, for uniform loads with corner supports, that yield zones extend laterally while the centre zone carries a negative moment.
- (4) The ultimate load approached that predicted for collapse. However, the non-linearity in the load deflection curves of the various joints suggest that the distribution of loads in the chords moves towards that predicted for the collapse state as a result of bolt slip or other sources of non-linearity, without actually buckling a chord member.

REFERENCES

REFERENCES

- [1] Wang Chu Kia, "General Computer Program for Limit Analysis", ASCE, J. Struct. Div., 89, ST6, December 1963, pp.101-117.
- [2] Shin Be, Y.K., "Automatic Limit Analysis of Triangulated Space Structures, J.Inst. Struc.Eng., 48, January 1970, pp.21-29.
- [3] Davis, R.M., "Space Structures", International Conference on Space Structures, University of Surrey, England, 1966.
- [4] Timoshenko, S., "Theory of Plates and Shells", McGraw-Hill, Inc., New York, N.Y., 1940.
- [5] Flower, William R., and Schmidt, Lewis, C., "Analysis of Space Truss as Equivalent Plate", ASCE, J. Struct. Div., 97, ST12, December, 1971, pp.2777-2789.
- [6] Suzuki, E., Kitamura, H., and Yamada, M., "The Analysis of the Space Truss Plate by Difference Equations", International Conference on Space Structures, University of Surrey, England, ed. by R.M.Davis, 1966, pp.136-144.
- [7] Flower, William R., and Schmidt, Lewis C., "Approximate Analysis of a Parallel-Chord Space Truss", Institution of Engineers, Australia, Civ.Eng.Trans., CE-13, April, 1971, pp.52-55.
- [8] Schmidt, L.C., "Alternative Design Methods for Parallel-Chord Space Trusses, J. Inst. Struc. Eng., 50, August 1972, pp.295-302.
- [9] Dickie, J.F., and Dunn, D.J., "Yield Pattern Considerations in Space Structures", J. Inst.Struc.Eng., 53, March, 1975, pp.147-152.
- [10] Mezzina, M., Prete, G., and Tosto, A., "Automatic and Experimental Analysis for a Model of Space Grid in Elastoplastic Behaviour", 2nd Internat. Conference on Space Structures, University of Surrey, England, September 1975, pp.570-588.
- [11] Marsh, C., "The Ultimate Strength of Orthogonal Grid Space Trusses", ASCE Nat. Convention, Montreal, 1974.

APPENDIX A

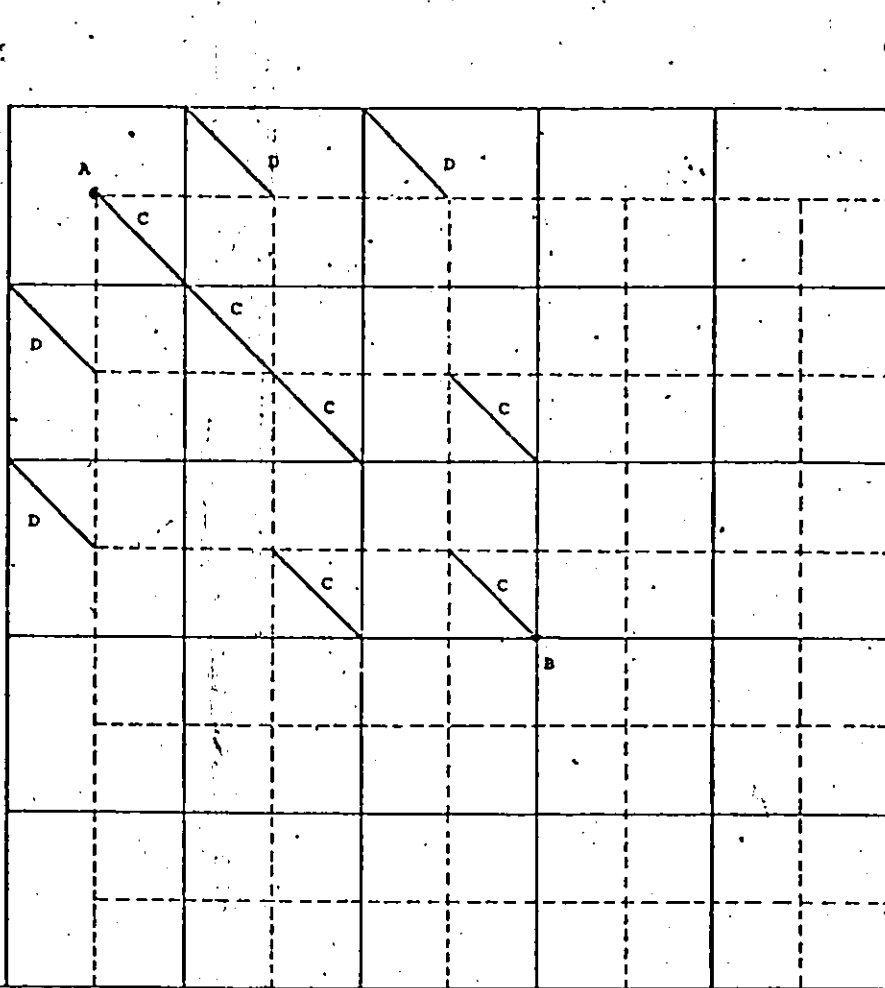


FIG. A.1 ILLUSTRATION OF THE REINFORCED DIAGONALS IN FIRST TEST MODEL (ONLY THE REINFORCED DIAGONALS ARE SHOWN)

Notation:

- C : Double diagonal with two bolts connection.
- D : Double diagonal with one bolt connection.

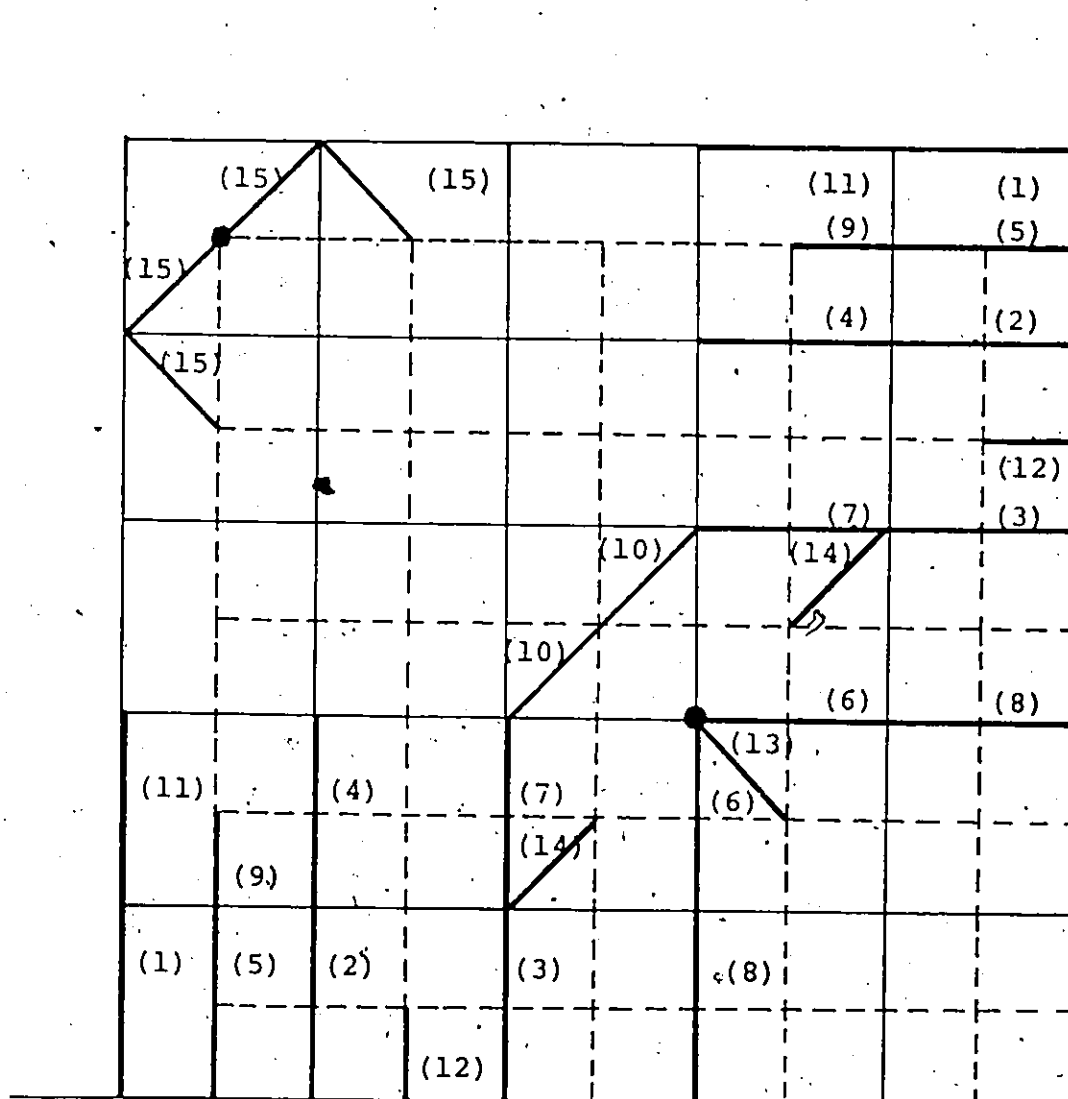


FIG. A.2 SEQUENCE OF MEMBER FAILURE FOR FIRST TEST MODEL ACCORDING TO ULTIMATE COMPUTER ANALYSIS

Failing load for 1st cycle = 30431 lb
 Failing load for 10th cycle = 39539 lb
 Failing load for 15th cycle = 40418 lb

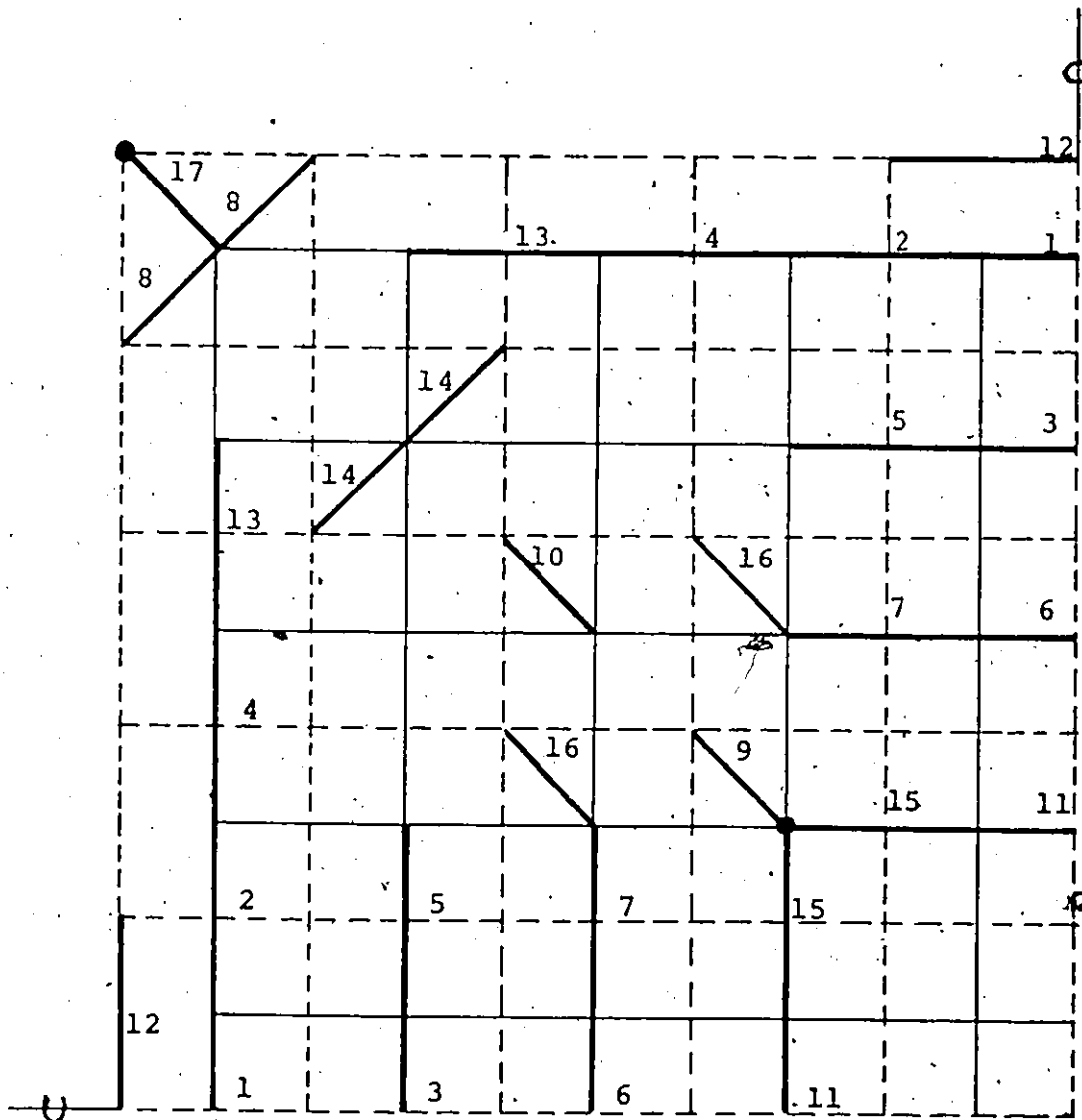


FIG. A.3 SEQUENCE OF MEMBER FAILURE FOR SECOND TEST MODEL ACCORDING TO ULTIMATE COMPUTER ANALYSIS (ONLY THE FAILING DIAGONALS ARE SHOWN)

Failing load at 1st cycle = 16532 lb.
 Failing load at 8th cycle = 23959 lb.
 Failing load at 17th cycle = 26849 lb.

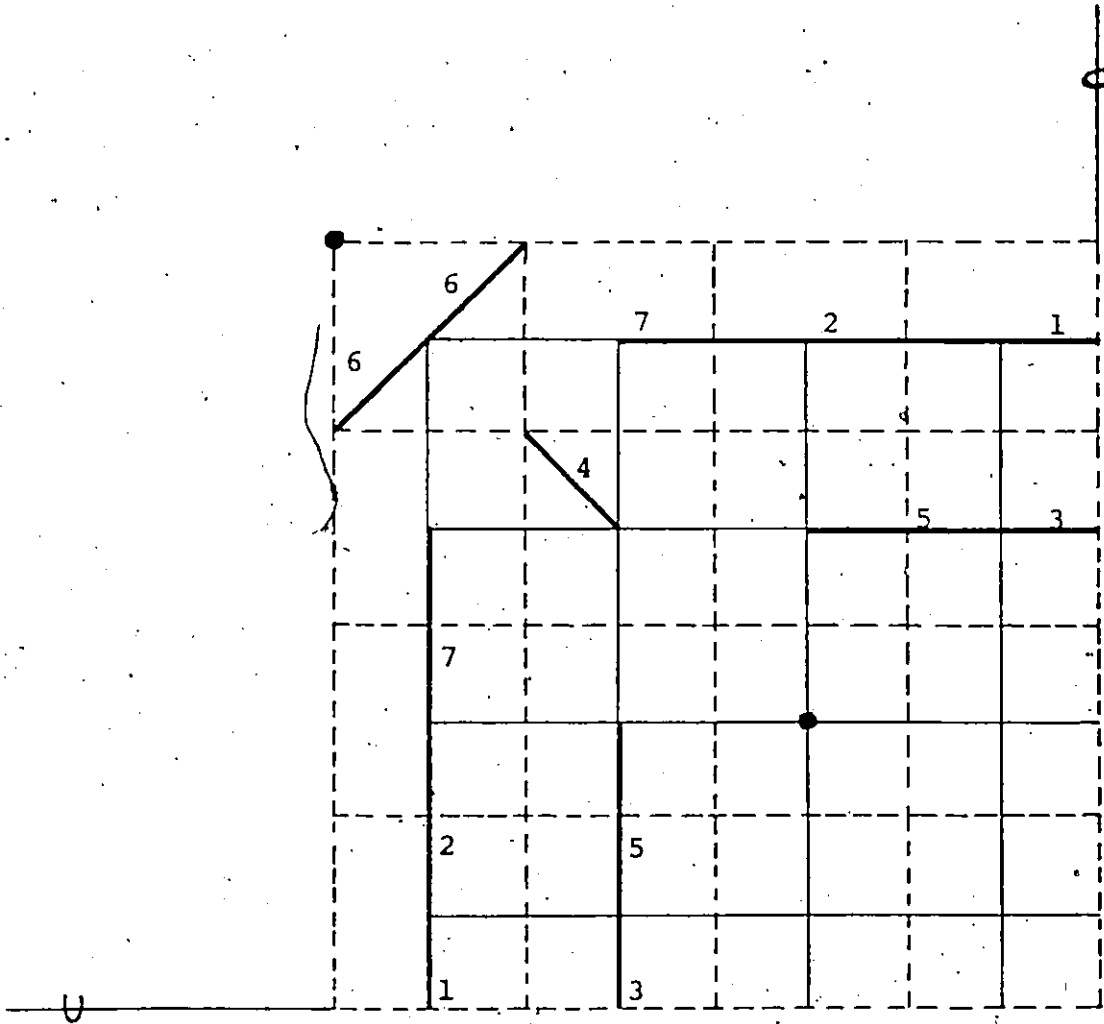


FIG. A.4 SEQUENCE OF MEMBER FAILURE FOR THIRD TEST MODEL ACCORDING TO ULTIMATE COMPUTER ANALYSIS (ONLY THE FAILING DIAGONALS ARE SHOWN)

Failing load at 1st cycle = 16858 lb.
 Failing load at 4th cycle = 23292 lb.
 Failing load at 7th cycle = 23964 lb.

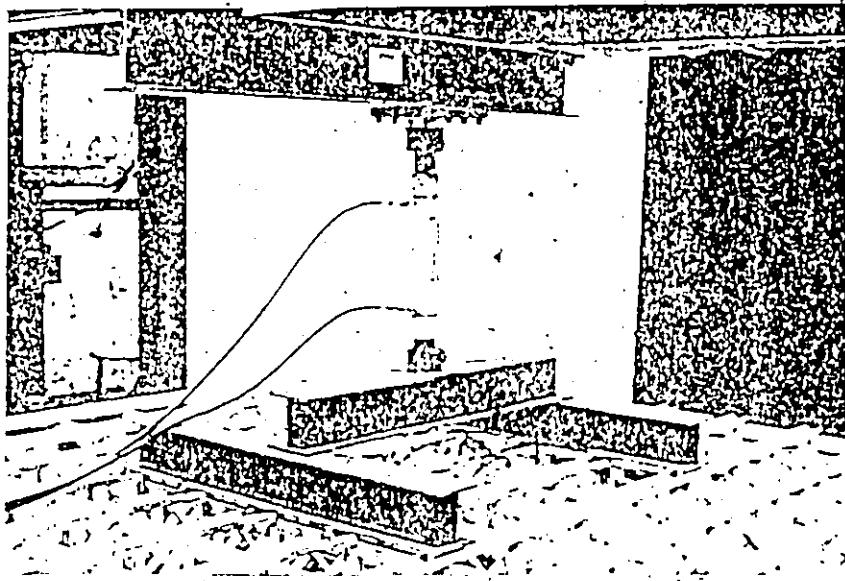


FIG. A.5 METHOD OF LOAD APPLICATION TO TEST MODEL

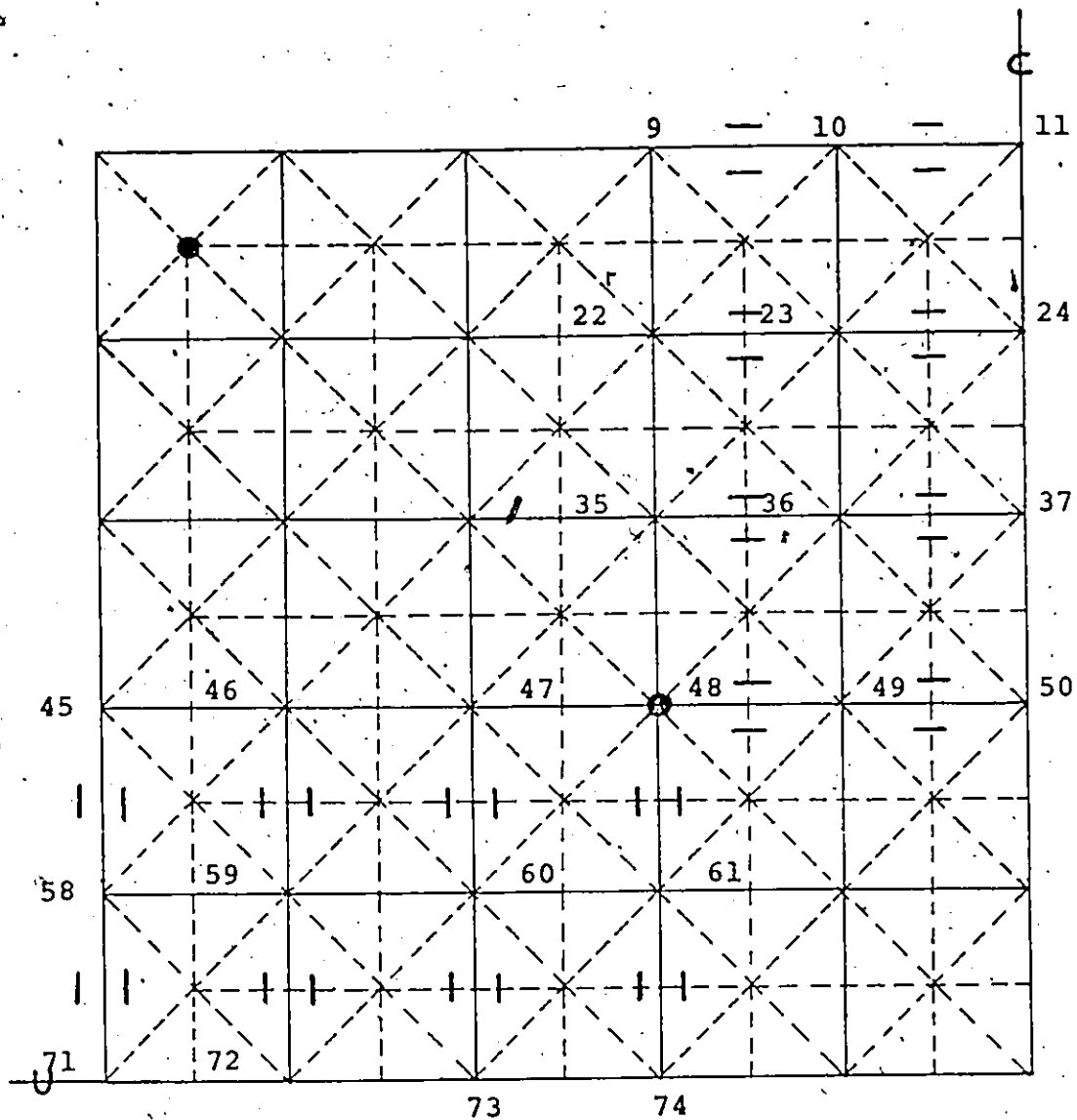


FIG. A.6 LOCATION OF STRAIN-GAGES IN FIRST TEST MODEL

TABLE A.1

Measured Vertical Deflections of Joints 45,
71, 48, 76, of First Test Model

Load (lb)	Vertical Deflection (in)			
	Joint 45	Joint 71	Joint 48	Joint 76
1	2	3	4	5
0.000	0.000	0.000	0.000	0.000
2454	0.021	0.049	0.066	0.050
4909	0.058	0.110	0.156	0.117
9818	0.1575	0.229	0.306	0.250
14727	0.255	0.349	0.466	0.400
19636	0.569	0.694	0.866	0.665
22090	0.769	0.921	1.116	0.775
24545	1.034	1.110	1.316	0.965
26999	1.117	1.317	1.556	1.172
29454	1.314	1.525	1.811	1.390
30681	1.469	1.669	1.981	1.525
31908	1.689	1.789	2.129	1.635

TABLE A.2

Strain-Gage Readings for Members Along
the Assumed Yield Lines of First Test
Model

Total Load in the Structure : 2454 lbs						
Members		Strains		Average Strain	Forces From Strains (lbs)	Forces From Com- puter Analysis (lbs)
End 1-End 2	Gage I	Gage II				
1	2	3	4	5	6	
9-10	97	97	97	391	482	
10-11	113	113	113	456	527	
22-23	113	97	105	424	472	
23-24	113	121	117	472	505	
35-36	94	70	82	327	368	
36-37	97	94	96	387	361	
48-49	47	82	64	258	321	
49-50	31	31	31	125	257	

(1)

Total Load in the Structure : 4909 lbs					
1	2	3	4	5	6
9-10	187	191	189	763	964
10-11	203	222	212	856	1054
22-23	250	222	236	953	944
23-24	250	253	252	1018	1010
35-36	187	156	171	690	736
36-37	191	183	187	755	722
48-49	113	156	134	541	642
49-50	82	82	82	331	534

(2)

Total Load in the Structure : 9818 lbs					
1	2	3	4	5	6
9-10	343	374	358	1446	1928
10-11	394	409	401	1620	2108
22-23	550	499	524	2116	1888
23-24	534	565	549	2217	2020
35-36	406	343	374	1510	1472
36-37	390	370	380	1535	1444
48-49	238	277	452	1826	1284
49-50	160	175	168	678	1068

(3)

Total Load in the Structure : 14727 lbs					
1	2	3	4	5	6
9-10	515	550	532	2149	2892
10-11	597	620	608	2456	3162
22-23	815	753	784	3167	2832
23-24	819	862	840	3393	3030
35-36	624	530	577	2331	2208
36-37	597	550	573	2314	2166
48-49	347	378	362	1462	1826
49-50	238	250	244	985	1602

(4)

TABLE A.2 (continued)

Total Load in the Structure : 19636 lbs					
1	2	3	4	5	6
9-10	628	729	678	2739	3856
10-11	753	737	745	3009	4216
22-23	1045	998	1021	4134	3776
23-24	1076	1154	1115	4504	4040
35-36	936	838	887	3583	2944
36-37	858	799	828	3345	2888
48-49	441	441	1441	1781	2568
49-50	296	316	306	1236	2136

(5)

Total Load in the Structure : 22090 lbs					
1	2	3	4	5	6
9-10	768	874	821	3316	4337
10-11	905	874	889	3591	4742
22-23	1186	1123	1154	4662	4247
23-24	1213	1295	1254	5066	4544
35-36	1045	924	984	3975	3311
36-37	955	905	930	3757	3248
48-49	503	472	487	1967	2888
49-50	316	347	331	1337	2402

(6)

TABLE A.2 (continued)

Total Load in the Structure : 24545 lbs					
1	2	3	4	5	6
9-10	874	987	930	3757	4820
10-11	987	971	979	3955	5270
22-23	1310	1275	1292	5219	4720
23-24	1345	1486	1415	5716	5050
35-36	1143	1030	1086	4387	3680
36-37	1061	1002	1031	4165	3610
48-49	562	499	530	2141	3210
49-50	347	374	360	1575	2670

(7)

Total Load in the Structure : 26999 lbs					
1	2	3	4	5	6
9-10	955	1076	1015	4100	5302
10-11	1076	1061	1068	4314	5796
22-23	1439	1392	1415	5716	5192
23-24	1498	1638	1568	6334	5554
35-36	1275	1186	1230	4969	4048
36-37	1189	1158	1173	4738	3971
48-49	624	534	579	2339	3531
49-50	378	409	393	1587	2937

(8)

TABLE A.2 (continued)

Total Load in the Structure : 29454 lbs					
1	2	3	4	5	6
9-10	1080	1201	1140	4605	5784
10-11	1217	1189	1203	4860	6324
22-23	1576	1517	1546	6245	5664
23-24	1626	1786	1706	6892	6059
35-36	1392	1345	1368	5526	4416
36-37	1342	1326	1334	5389	4332
48-49	651	565	608	2456	3852
49-50	406	433	419	1692	3204

(9)

Total Load in the Structure : 30681 lbs					
1	2	3	4	5	6
9-10	1174	1264	1219	4924	5996
10-11	1264	1271	1267	5118	6500
22-23	1626	1548	1587	6411	5947
23-24	1685	1860	1772	7158	6427
35-36	1459	1420	1439	5813	4589
36-37	1404	1404	1404	5672	4497
48-49	686	581	633	2557	3920
49-50	413	452	432	1745	3216

(10)

TABLE A.2 (continued)

Total Load in the Structure : 31908 lbs					
1	2	3	4	5	6
9-10	1228	1334	1281	5175	6032
10-11	1310	1345	1327	5361	6500
22-23	1720	1650	1685	6807	6091
23-24	1771	1969	1870	7554	6500
35-36	1486	1498	1492	6027	5076
36-37	1439	1498	1468	5930	5117
48-49	694	624	659	2662	4180
49-50	437	472	454	1834	3465

(11)

TABLE A.2 (continued)

TABLE A.3

Vertical Deflections for Joints 45, 71,
48, 76 of First Model According
to Computer Analysis

Cycles ⁽¹⁾	Load (lb)	Deflection (in)			
		Joint 45	Joint 71	Joint 48	Joint 76
1	30431	0.414	0.560	0.710	0.770
2	31037	0.426	0.577	0.728	0.789
3	34418	0.558	0.784	0.908	0.973
4	37042	0.763	1.119	1.187	1.268
5	37070	0.765	1.122	1.190	1.271
6	37333	0.792	1.168	1.226	1.309
7	37432	0.807	1.195	1.248	1.333
8	37849	0.881	1.326	1.359	1.451
9	38786	1.077	1.480	1.487	1.592
10	39539	1.254	1.773	1.742	1.870

(1) Each cycle gives the load increment for the next strut failure.

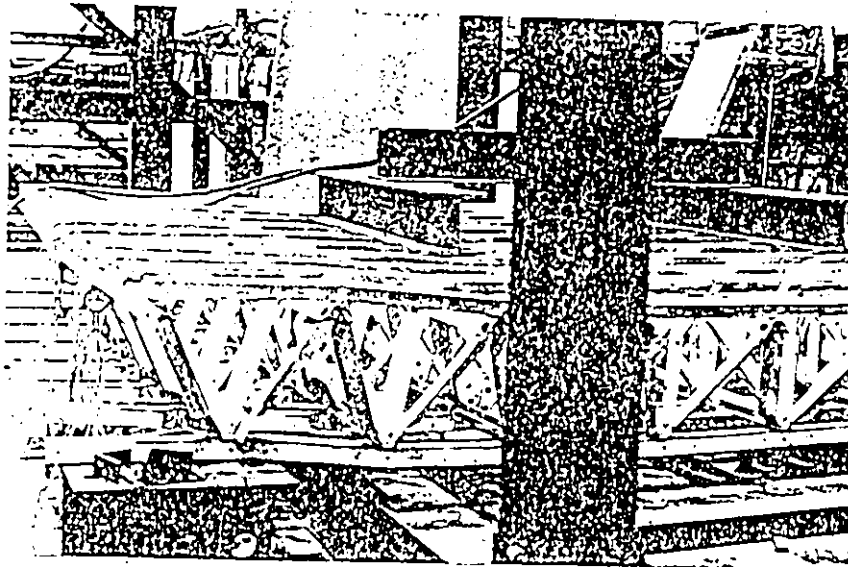


FIG. A.7 FAILURE OF FIRST TEST MODEL

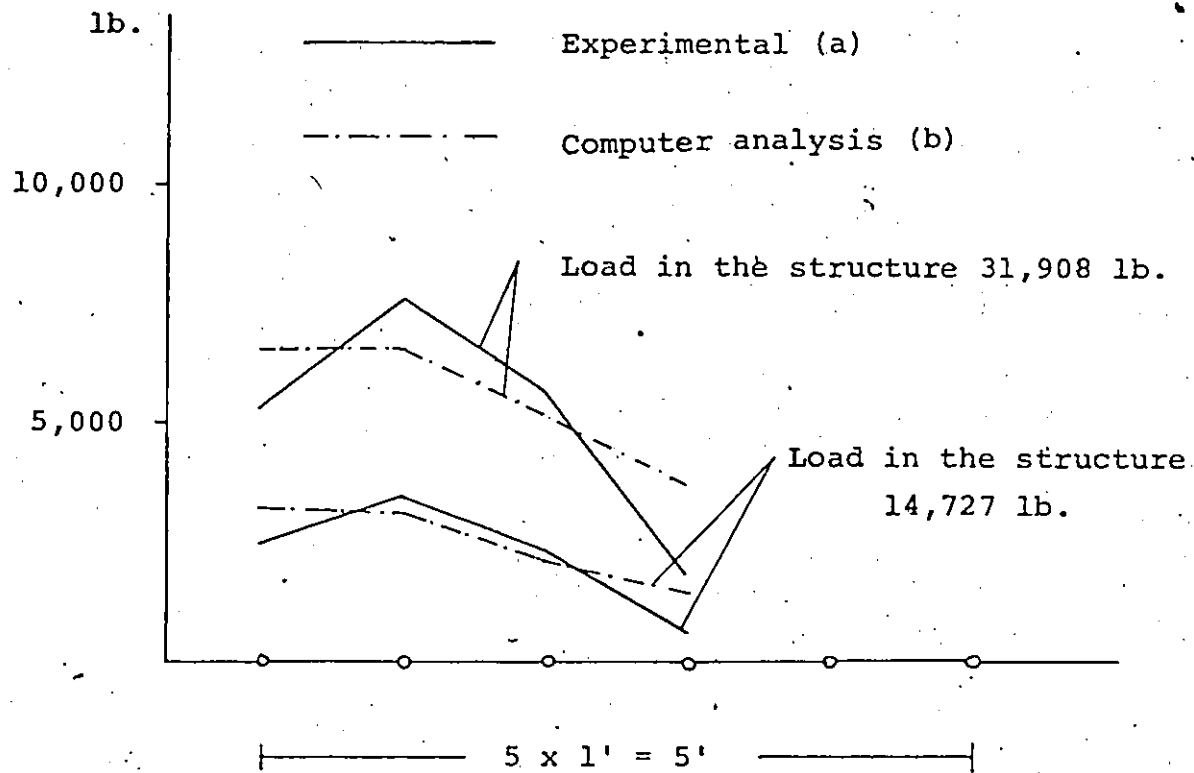


FIG. A.8 FORCES IN THE MEMBERS ALONG THE ASSUMED YIELD LINES OF THE FIRST TEST MODEL

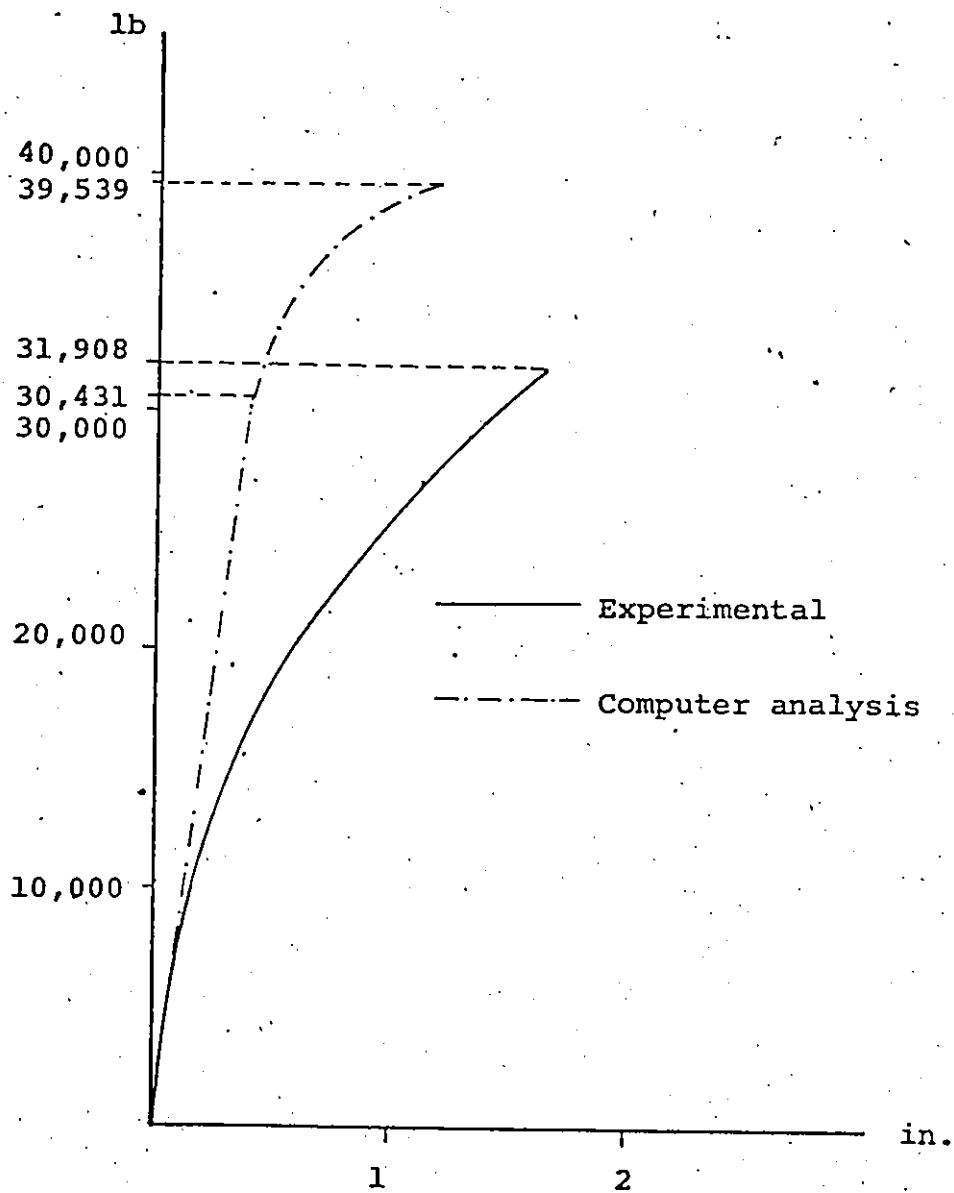


FIG. A.9 LOAD VERTICAL DEFLECTION CURVES FOR JOINT 45
OF FIRST TEST MODEL

(1)

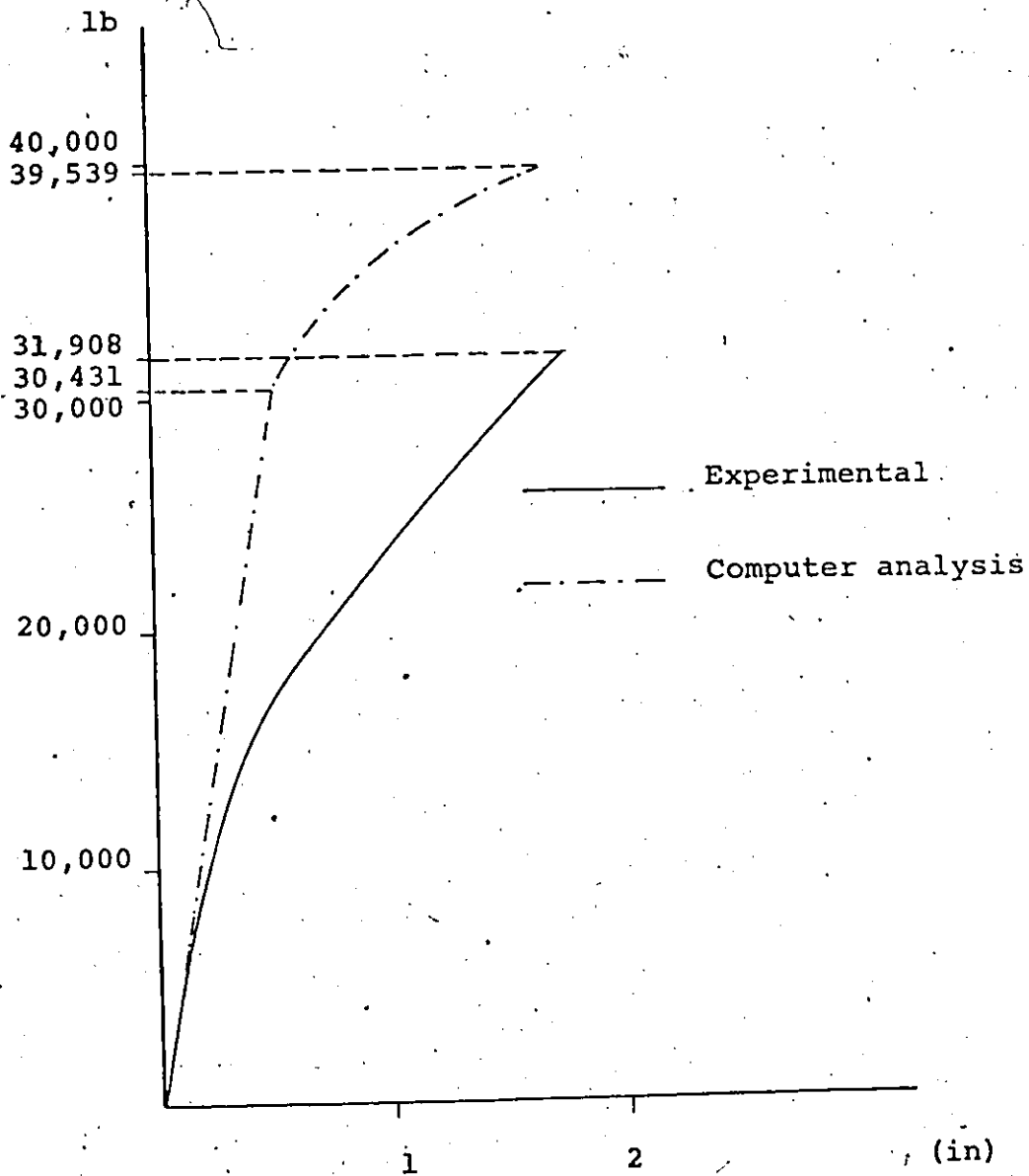


FIG. A.9 LOAD VERTICAL DEFLECTION CURVES FOR JOINT 71 OF FIRST TEST MODEL

(2)

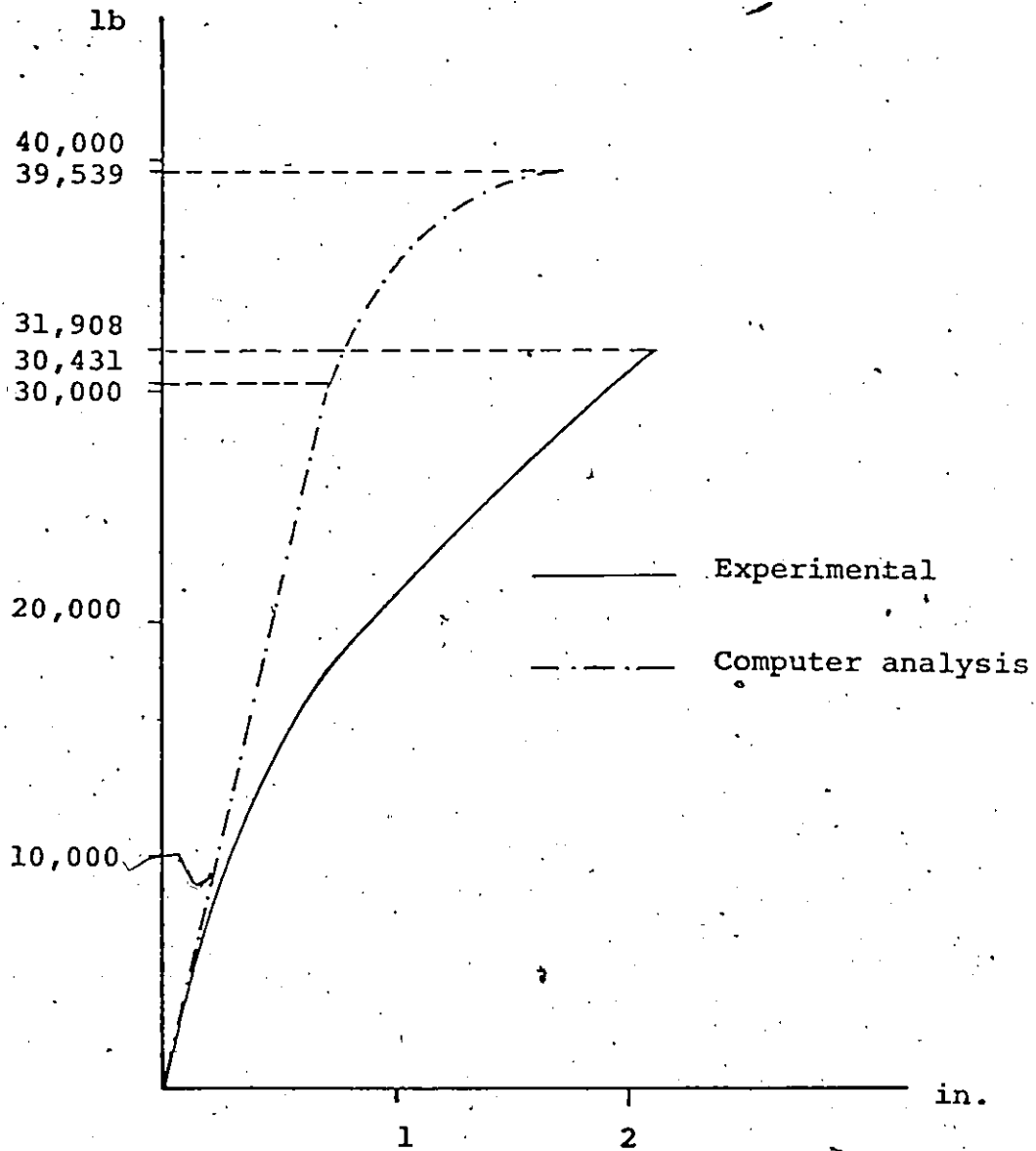


FIG. A.9 LOAD VERTICAL DEFLECTION CURVES FOR JOINT 48
OF FIRST TEST MODEL

(3)

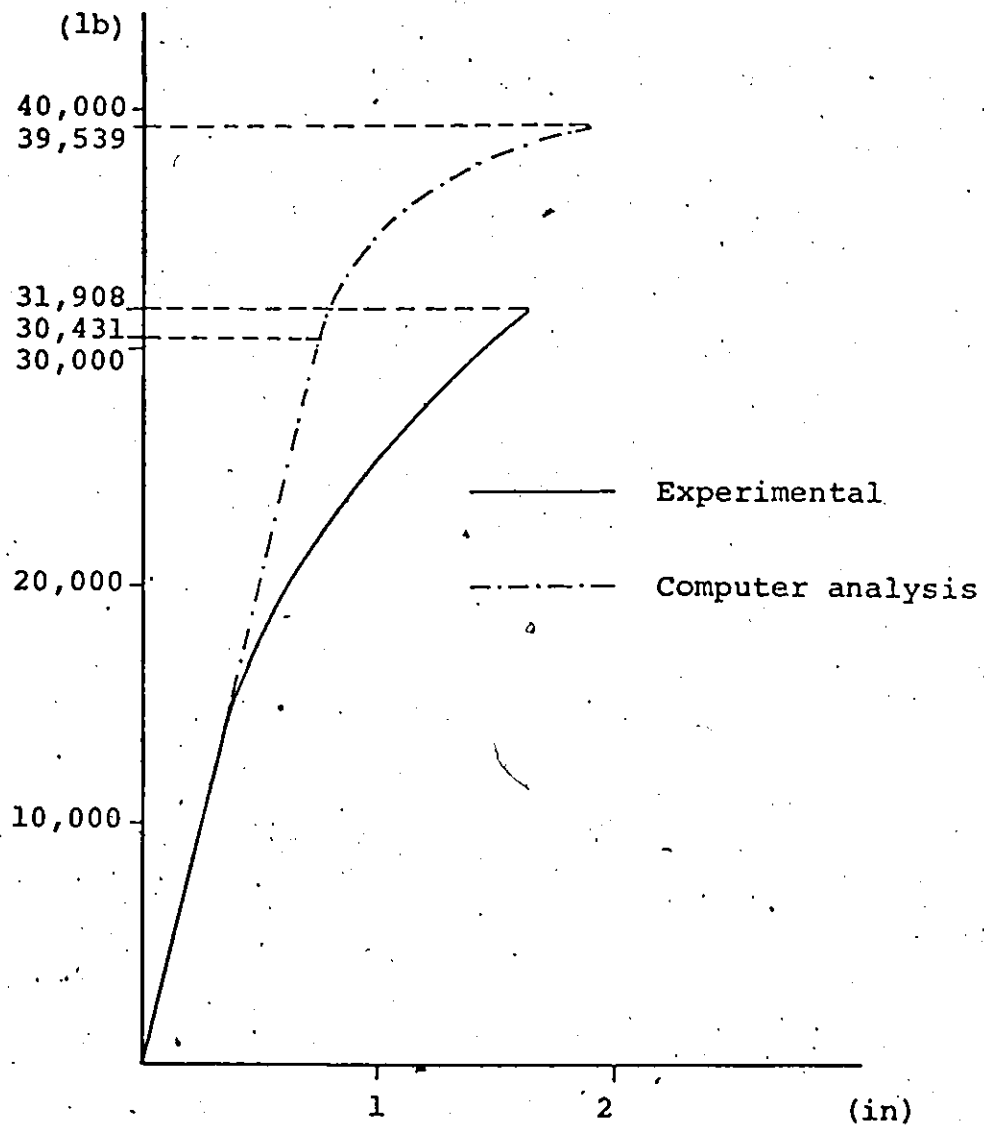


FIG. A.9. LOAD VERTICAL DEFLECTION CURVES FOR JOINT 76
OF FIRST TEST MODEL

(4)

TABLE A.4

Measured Vertical Deflections of Joints 45, 71,
55, 76, of Second Model

Load (lb)	Vertical Deflection (in)			
	Joint 45	Joint 71	Joint 55	Joint 76
1	2	3	4	5
0	0	0	0	0
2450	0.102	0.105	0.242	0.140
4909	0.224	0.241	0.417	0.330
7350	0.375	0.412	0.632	0.550
9800	0.557	0.615	0.857	0.780
12250	0.744	0.815	1.097	1.030
13475	0.862	0.915	1.267	1.220
14700	0.939	1.005	1.377	1.340
15925	1.044	1.117	1.532	1.500
17150	1.144	1.230	1.682	1.650
18375	1.334	1.375	1.792	1.850

TABLE A.5

Vertical Deflections of Joints 45, 71,
76, 55, Second Model According
to Computer Analysis

Load (lb)	Vertical Deflection (in)			
	Joint 45	Joint 71	Joint 55	Joint 76
1	2	3	4	5
16532	0.528	0.628	0.778	0.758
17977	0.599	0.728	0.874	0.853
19370	0.677	0.827	0.976	0.954
20975	0.826	1.047	1.171	1.149
21493	0.886	1.130	1.245	1.223
22202	0.974	1.238	1.352	1.329
23949	1.292	1.694	1.782	1.749
23959	1.294	1.696	1.789	1.751

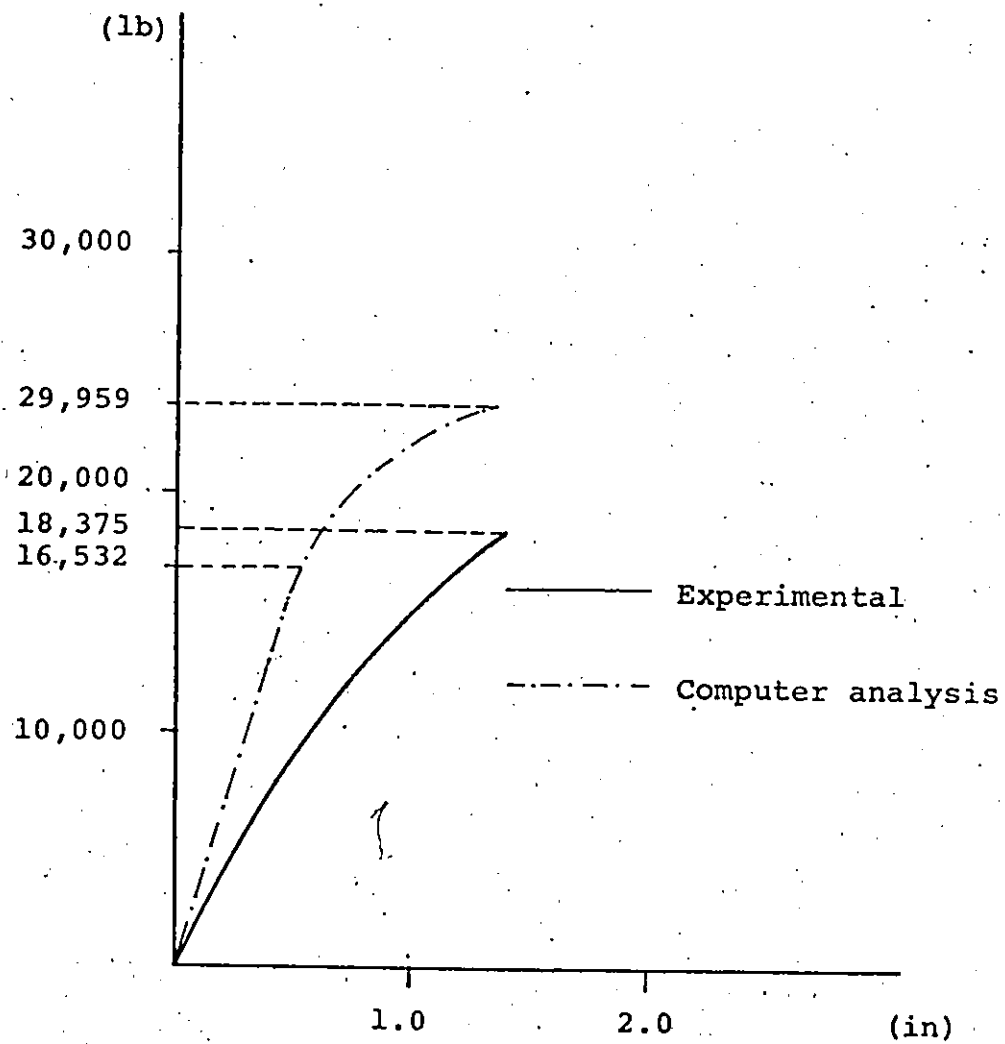


FIG. A.10 LOAD VERTICAL DEFLECTION CURVES FOR JOINT 45 OF SECOND TEST MODEL

(1)

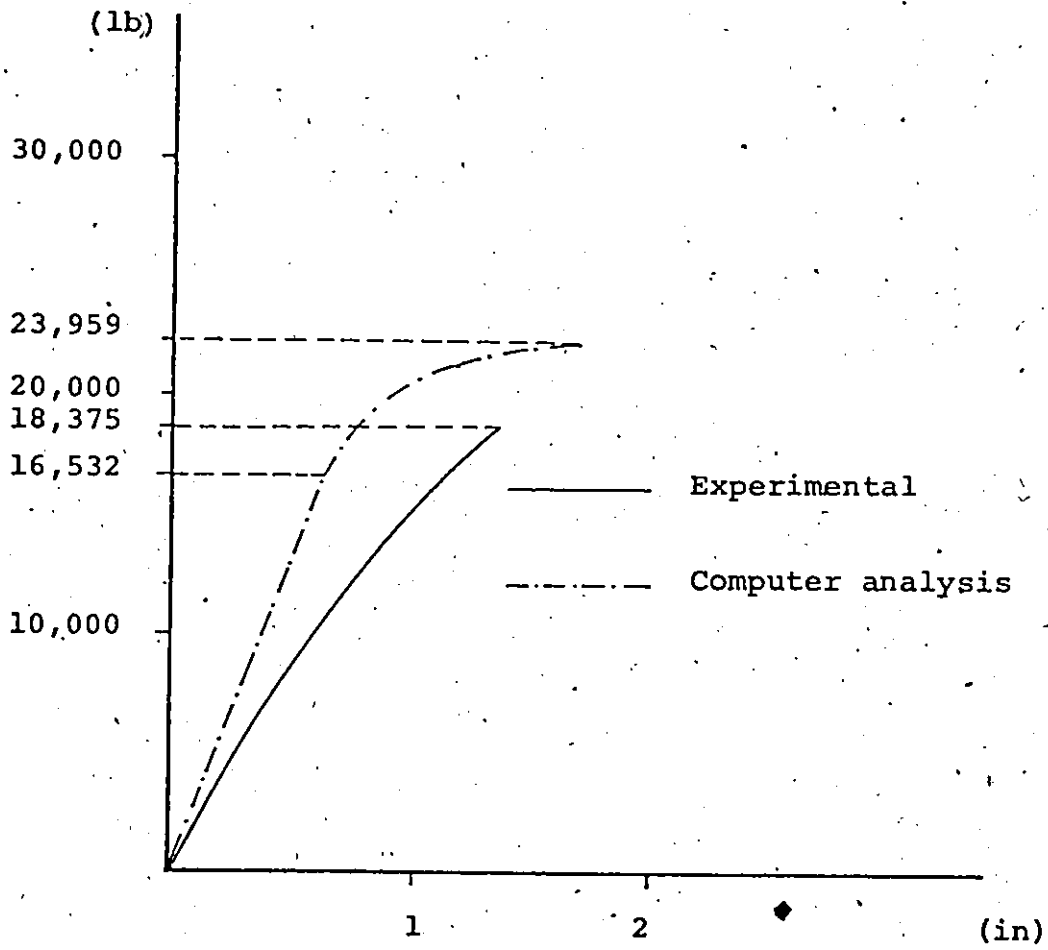


FIG. A.10 LOAD VERTICAL DEFLECTION CURVES FOR JOINT 71
OF SECOND TEST MODEL

(2)

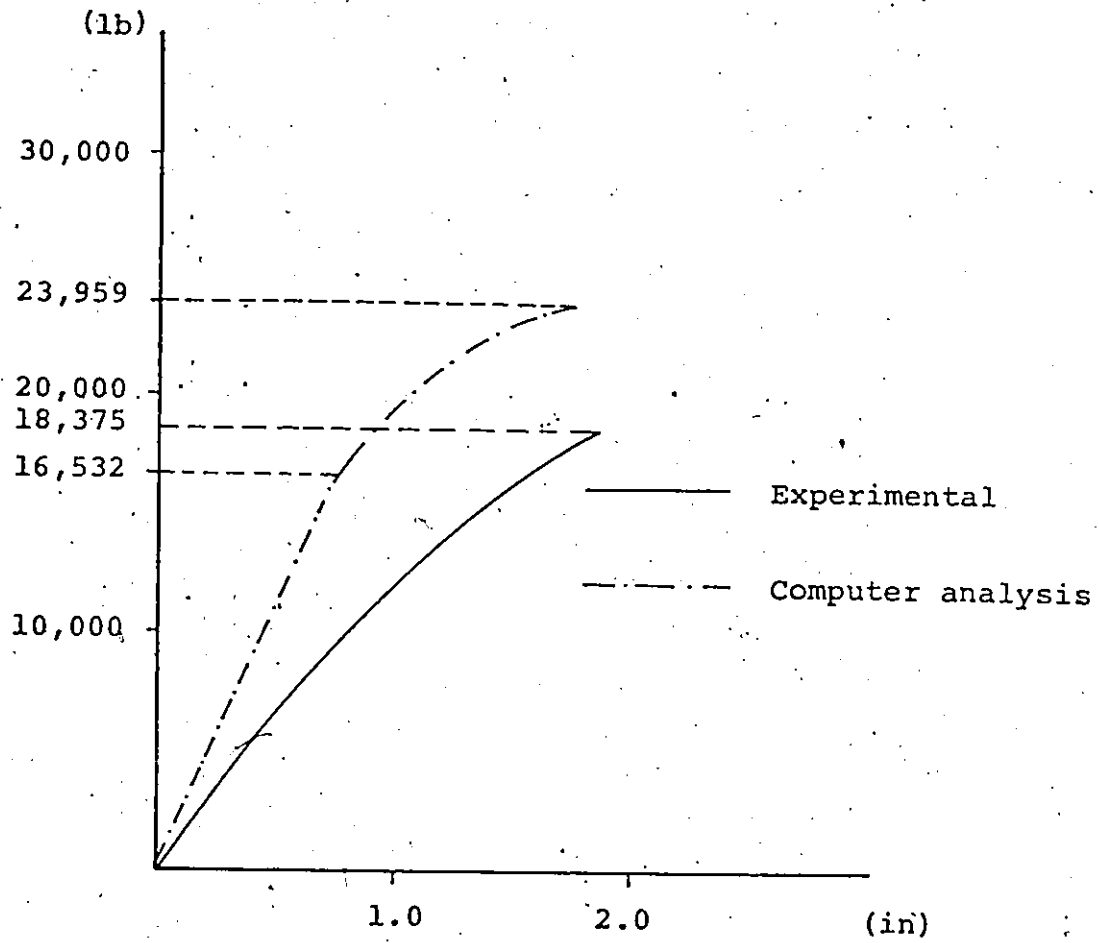


FIG. A.10 LOAD VERTICAL DEFLECTION CURVES FOR JOINT 55
OF SECOND TEST MODEL

(3)

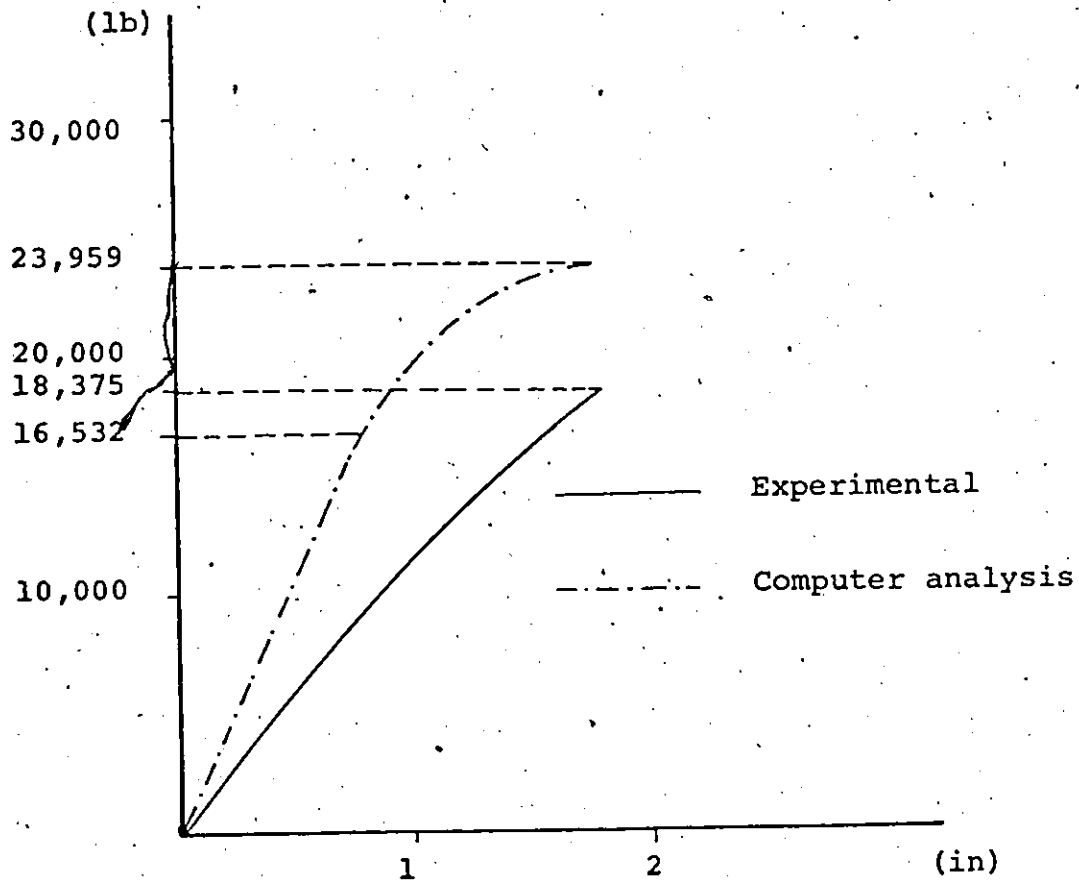


FIG. A.10 LOAD VERTICAL DEFLECTION CURVES FOR JOINT 76 OF SECOND TEST MODEL

(4)

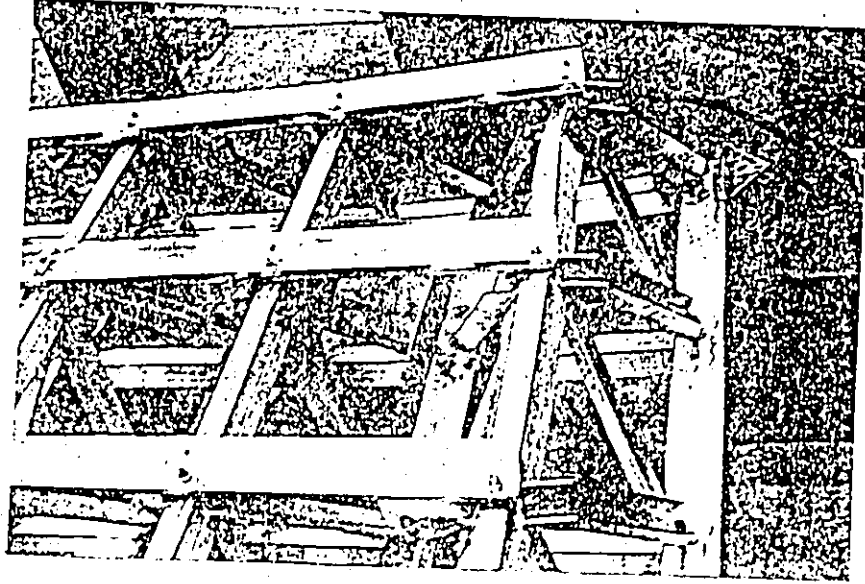


FIG. A.11' FAILURE OF SECOND TEST MODEL

TABLE A.6

Vertical Deflections of Joints 27, 49,
35, 53, of Third Model According
to Computer Analysis

Load (lb)	Vertical Deflection (in)			
	Joint 27	Joint 49	Joint 35	Joint 53
1	2	3	4	5
16856	0.325	0.430	0.506	0.490
18865	0.395	0.547	0.610	0.593
21660	0.516	0.718	0.780	0.761
23292	0.638	0.928	0.963	0.951

TABLE A.7

Measured Vertical Deflections of Joints
27, 49, 35, 53, of Third Model

Load (lb)	Vertical Deflection (in)			
	Joint 27	Joint 49	Joint 35	Joint 53
1	2	3	4	5
0	0	0.000	0.000	0.000
2450	0.055	0.070	0.090	0.082
4900	0.160	0.200	0.232	0.230
9800	0.380	0.490	0.550	0.572
12250	0.530	0.685	0.732	0.756
14700	0.710	0.875	0.960	0.985
15925	0.800	0.950	1.075	1.080
17150	0.885	1.040	1.195	1.220
18375	1.025	1.195	1.340	1.380
19600	1.140	1.330	1.490	1.530
20825	1.290	1.500	1.680	1.720
22050	1.420	1.665	1.840	1.880

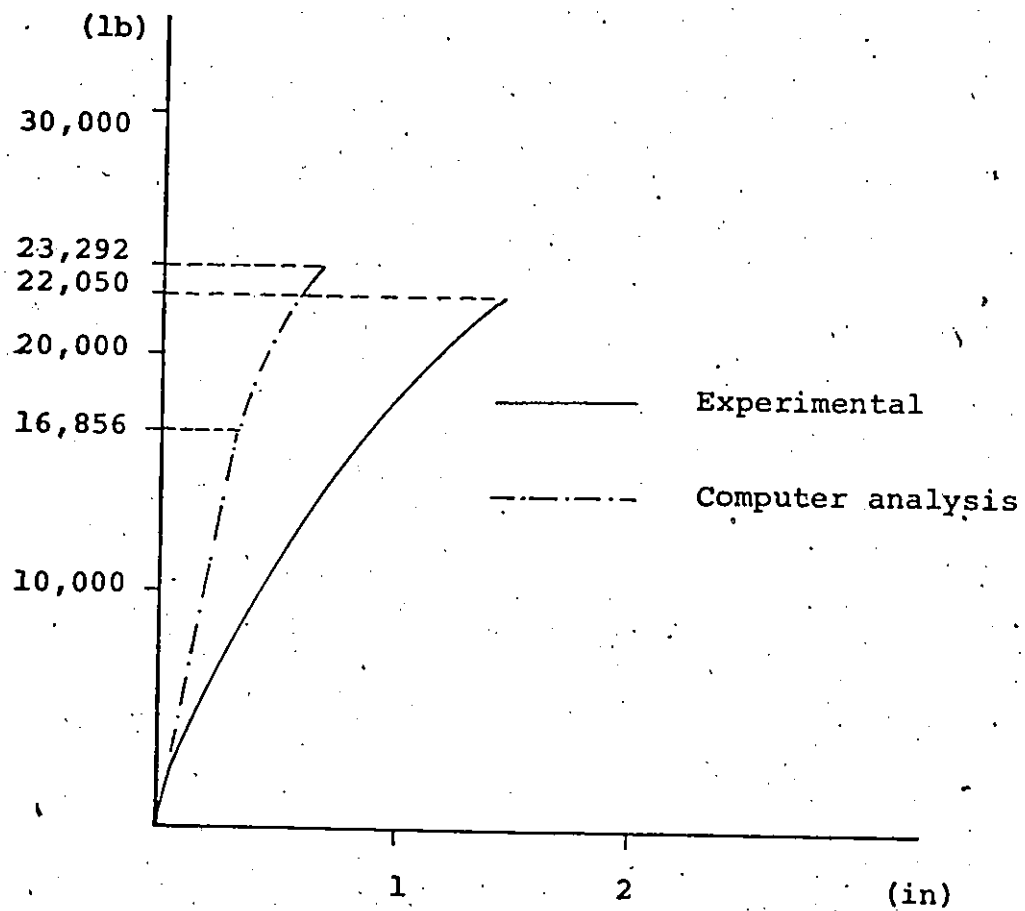


FIG. A.12 LOAD VERTICAL DEFLECTION CURVES FOR JOINT 27
OF THIRD TEST MODEL

(1)

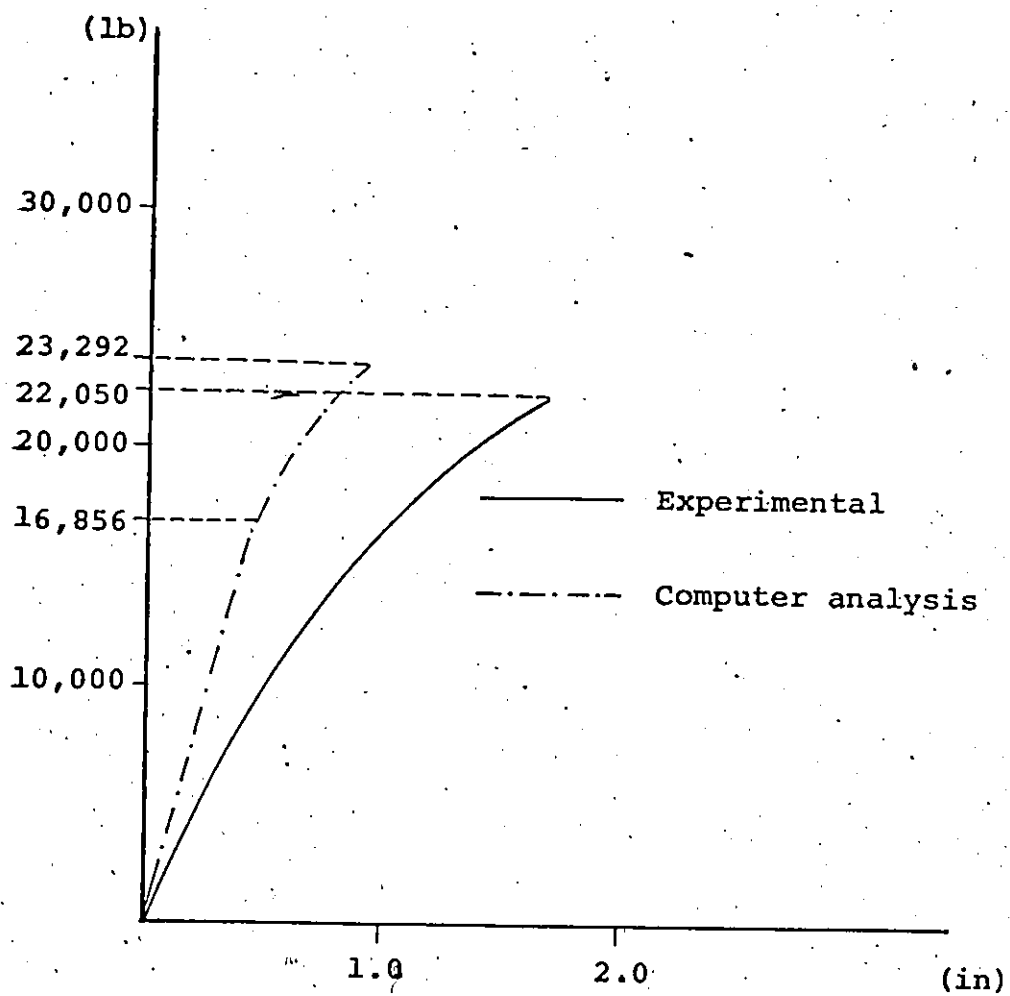


FIG. A.12 LOAD VERTICAL DEFLECTION CURVES FOR JOINT 49
OF THIRD TEST MODEL

(2)

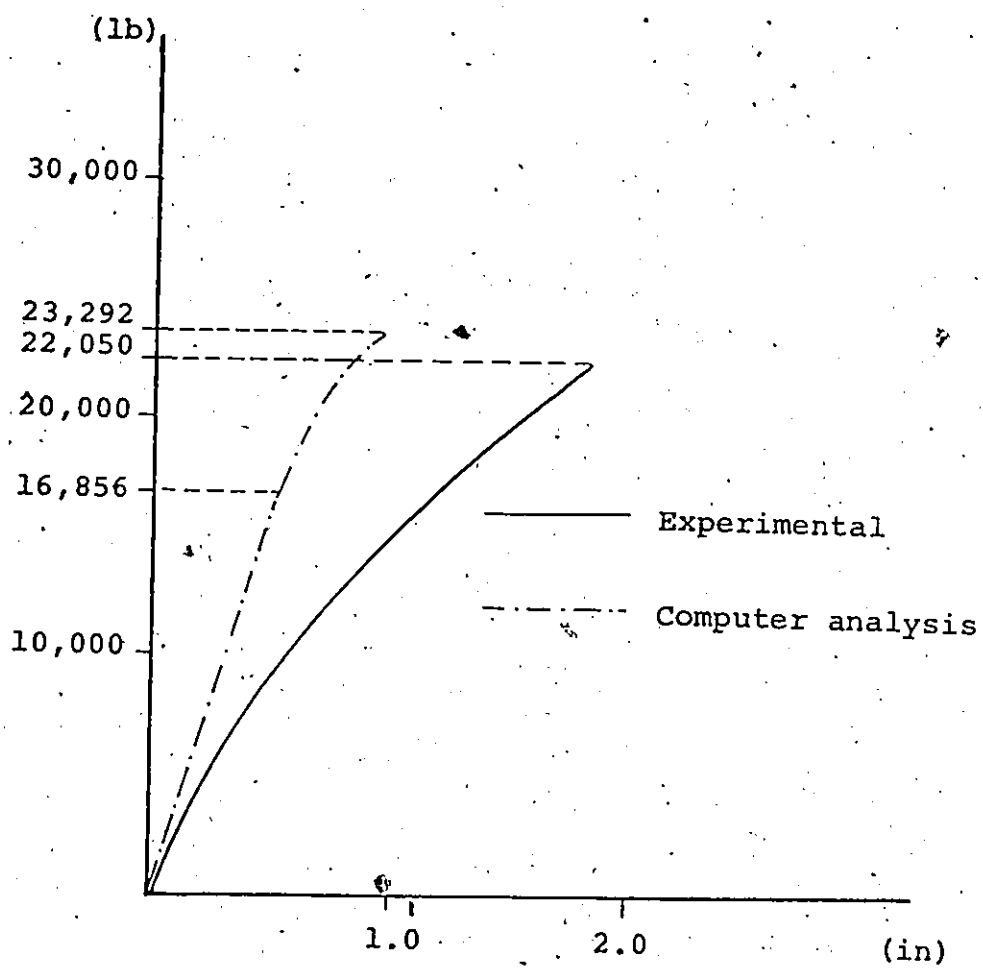


FIG. A.12 LOAD VERTICAL DEFLECTION CURVES FOR JOINT 35.
OF THIRD TEST MODEL

(3)

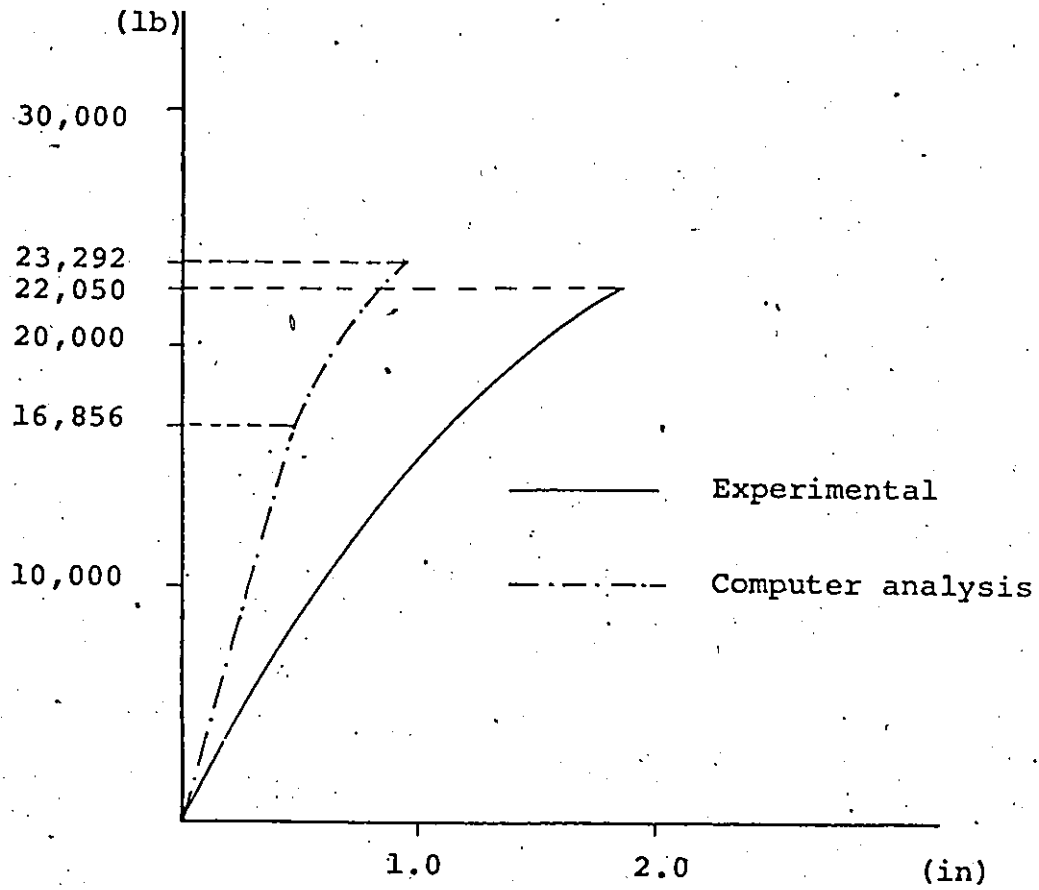


FIG. A.12 LOAD VERTICAL DEFLECTION CURVES FOR JOINT 53 OF THIRD TEST MODEL

(4)